

Journal Pre-proofs

Extended Integrated Force Method for the analysis of prestress-stable statically and kinematically indeterminate structures

Yafeng Wang, Gennaro Senatore

PII: S0020-7683(20)30202-X
DOI: <https://doi.org/10.1016/j.ijsolstr.2020.05.029>
Reference: SAS 10732

To appear in: *International Journal of Solids and Structures*

Received Date: 16 December 2019
Revised Date: 17 April 2020
Accepted Date: 21 May 2020

Please cite this article as: Y. Wang, G. Senatore, Extended Integrated Force Method for the analysis of prestress-stable statically and kinematically indeterminate structures, *International Journal of Solids and Structures* (2020), doi: <https://doi.org/10.1016/j.ijsolstr.2020.05.029>

This is a PDF file of an article that has undergone enhancements after acceptance, such as the addition of a cover page and metadata, and formatting for readability, but it is not yet the definitive version of record. This version will undergo additional copyediting, typesetting and review before it is published in its final form, but we are providing this version to give early visibility of the article. Please note that, during the production process, errors may be discovered which could affect the content, and all legal disclaimers that apply to the journal pertain.

© 2020 Elsevier Ltd. All rights reserved.



Extended Integrated Force Method for the analysis of prestress-stable statically and kinematically indeterminate structures

Yafeng WANG, Gennaro SENATORE*

Applied Computing and Mechanics Laboratory (IMAC), School of Architecture, Civil and Environmental Engineering (ENAC), Swiss Federal Institute of Technology (EPFL), CH-1015 Lausanne, Switzerland
yafeng.wang@epfl.ch, gennaro.senatore@epfl.ch

Abstract

This paper presents a new force method to predict the structural response of statically and kinematically indeterminate systems that can be stabilized through prestress, i.e. prestress-stable structures. This new force method, here named Extended Integrated Force Method (IFME), extends the existing Integrated Force Method (IFM) which is only applicable to the analysis of kinematically determinate systems. The product force concept is adopted and incorporated into the IFME to model the effect of infinitesimal mechanisms. This makes the IFME capable of dealing with cases in which the external loads contain components that cannot be taken by the system in its initial configuration. As the original IFM, the IFME bypasses the well-known concept of redundant forces and basis determinant structure of the Standard Force Method (SFM) by taking the internal forces as the independent variables which are obtained simultaneously. A proof is provided to show that, when the product force is not included in the formulation, the IFME reduces to the IFM for kinematically determinate systems and it also reduces to another force method based on singular value decomposition of the equilibrium matrix which is here named SVD-FM. Compared to the better known Displacement Method (DM), the IFME is a suitable alternative and it offers a deeper insight into the structure response which is decoupled into an extensional and an inextensional part for prestress-stable kinematically indeterminate systems. Numerical examples are carried out to test accuracy and effectiveness of the IFME on kinematically indeterminate structures with multiple self-stress states and mechanism modes. Application of the IFME to active structural control of kinematically indeterminate systems is also discussed through a numerical example.

Keywords: Force Method; Integrated Force Method; Prestress-stable; Kinematically Indeterminate Systems; Active structural control

1 Introduction

The behavior of a reticular structural system can be characterized by two key parameters [1]: the number of zero-energy deformation modes, or mechanisms, denoted by m ; and the number of self-stress states, denoted by s . Structural systems can be classified into four types based on m and s : (1) statically determinate and kinematically determinate ($s = 0, m = 0$); (2) statically indeterminate and kinematically determinate ($s > 0, m = 0$); (3) statically determinate and kinematically indeterminate ($s = 0, m > 0$); (4) statically indeterminate and kinematically indeterminate ($s > 0, m > 0$). Most engineering structures fall into the first two types, i.e. kinematically determinate systems.

Although most engineering structures are kinematically determinate systems, kinematically indeterminate systems are not uncommon and have been applied in civil engineering in the form of cable domes [2, 3, 4], cable nets [5, 6, 7] and tensegrity structures [8, 9, 10]. These structures fall into the fourth category type, i.e. statically indeterminate and kinematically indeterminate systems. The existence of kinematic indeterminacy makes the analysis of the structural response more challenging because the displacements cannot be uniquely determined solely through equilibrium and compatibility conditions. Due to the presence of mechanisms, it is possible that the external load might contain components that cannot be equilibrated by the structure in its initial configuration. This occurs when load components lie in the left-null space of the equilibrium matrix which is spanned by the mechanism basis. In these cases, the equilibrium equations admit no solution.

Mechanisms can be distinguished into two main types: infinitesimal and finite mechanisms. It is well known that the only way a state of self-stress can impart first order stiffness to an inextensional mechanism is due to a second order change of strain energy caused by second order deformations of the structure elements [11, 12]. In this case, the change of geometry caused by the inextensional mechanism, can enable the pre-stressed elements to balance the external load that excites the mechanism. Therefore, prestress can be appropriately assigned to stabilize first-order infinitesimal mechanisms but not higher order or finite mechanisms. Kinematically indeterminate systems containing only first-order infinitesimal mechanisms that can be stabilized through prestress are usually referred as ‘prestress-stable’ [13]. Methods to evaluate whether a kinematically indeterminate system is prestress-stable have been proposed, among others, by Calladine and Pellegrino [14], Kuznetsov [15] and Tarnai and Szabo [16].

In [14], the main criterion to assess prestress stability was based on the effect of self-stress on the stiffness of the mechanism through the so-called ‘product forces’ which arise at the joints when a mechanism is excited. Through appropriate prestress, the product forces can equilibrate the load that has excited the mechanism, which otherwise could not be taken by the structure in its original configuration. In [15], another prestress stability criterion was formulated based on kinematic constraint functions and virtual displacements. Tarnai and Szabo [16] unified and proved equivalence of the prestress stability criteria given in [14] and [15] through the formulation of a more general theory based on stationarity of the Hellinger-Reissner variational principle.

As shown by Tarnai and Szabo [16], Calladine and Pellegrino [14] and Kuznetsov [15] arrive to the identical conclusion that if a state of self-stress or combination of multiple states (when they exist) can impart positive stiffness to all mechanisms in the assembly, then the mechanisms are first-order infinitesimal and the structure can be stabilized through prestress. This criterion involves to verify the positive definiteness of a quadratic form which contains the mechanisms modes, and the self-stress states. Although the works in [14, 15, 16] gave general criteria for prestress stability, they did not offer a general and efficient numerical procedure to obtain an appropriate prestress when the structure has multiple self-stress states. The task is to obtain a suitable combination of the self-stress states subject to appropriate constraints including the positive definiteness of any of the quadratic forms given in [14, 15, 16]. This task has been formulated through optimization procedures based on genetic algorithm [17], simulating annealing [18], ant colony algorithm [19], and semidefinite programming [20], which have adopted the criterion given in [14].

Once prestress stability condition is met and as a result an appropriate prestress is determined, a suitable method is needed to analyze the structural response under external loads. Structural analysis methods can be generally divided into two categories: displacement method (DM) (or stiffness method) and force method (FM) (or flexibility method). Within a Finite Element formulation, a structure is modelled as a mesh of elements connected at nodes. Both methods consider equilibrium and compatibility conditions. DM has been extensively used in structural analysis. The primal unknown variables are the node displacements. The so-called structure tangent stiffness consists of material and geometric stiffness. The material stiffness incorporates equilibrium and compatibility conditions for the structure in its initial unstressed configuration (i.e. it is assumed that the load does not cause a significant change of the geometry) while the geometric stiffness is employed to account for the stiffness caused

by a change of orientation of the stressed elements [21]. In FM, the primal unknown variables are the element forces. There are three main force method formulations: Standard Force Method (SFM) [22, 23, 24], Integrated Force Method (IFM) [25, 26, 27], and a Force Method based on Singular Value Decomposition [28] which is referred as SVD-FM in this paper.

For statically determinate structures, equilibrium conditions are sufficient to compute the unknown element forces. For statically indeterminate structures, equilibrium conditions are not sufficient to determine a unique solution because of the existence of redundant elements. Therefore, equilibrium conditions must be augmented by compatibility conditions. In the SFM, a statically indeterminate and kinematically determinate structure is first subdivided into a statically determinate basis structure and some redundant members. The element forces in the determinate basis structure can be obtained directly through equilibrium conditions; then the redundant forces are obtained through a back-substitution through compatibility conditions. This procedure was originally developed by Navier [29] to analyze statically indeterminate and kinematically determinate trusses.

The IFM was first proposed by Patnaik [25] for static analysis and it was subsequently developed further to address various analysis including stability [30] and structural dynamics [31]. In addition, it has been employed in structural optimization [32, 33] and integrated structure-control design [34]. Different to the SFM, the IFM combines equilibrium and compatibility into a single matrix statement thus allowing to compute the element forces directly without the need to choose any determinate basis structure nor redundant members. This is a significant advantage with respect to the SFM which can be thought of as derived from the IFM [30]. However, in its current form, the IFM cannot be applied to the analysis of structures with kinematic indeterminacies because it does not account for the change of stiffness caused by prestress and therefore it cannot compute the effect of mechanisms on forces and displacements in prestress-stable configurations.

Another force method, which was first formulated in [12, 28], is based on Singular Value Decomposition (SVD) of the equilibrium conditions in matrix form. For brevity, this method is referred here as SVD-FM. Appendix A.1 gives the key equations of this method. In the SVD-FM, the equilibrium matrix is decomposed through SVD into submatrices which contain complete information regarding static and kinematic properties including self-stress states and mechanism modes. Element forces and node displacements can be computed by combining these submatrices together with compatibility conditions. That being said, the

SVD-FM cannot be used to compute forces and displacements for kinematically indeterminate systems when the load lies in the left-null space of the equilibrium matrix i.e. when the load cannot be taken by the structure in its initial configuration because it excites one or more mechanisms.

Pellegrino [35] formulated a method to analyze reticular structures with kinematic indeterminacies by extending the SFM with the ‘product force’ or ‘geometric load’ method. The product force offers a way to compute the stiffness of a first-order infinitesimal mechanism which is developed as the mechanism is actuated and it results from application of prestress [36, 37]. By combining the product force matrix and the column space of the equilibrium matrix, a new equilibrium matrix was constructed; then a similar procedure as in the SFM was carried out to compute the element forces and nodal displacements. Although this method can be used to predict the structural response of prestress-stable statically and kinematically indeterminate systems, since they are based on the SFM, automation through software implementation is cumbersome and do not generalize well.

Reksowardojo and Senatore [38] proved that the SVD-FM and IFM are identical for kinematically determinate systems. Part of the conclusions in [38] is that the SVD-FM has generally a lower degree of computational complexity with respect to the IFM, the more so as the structure static indeterminacy increases. However, the IFM has a more intuitive formulation that is preferable pedagogically and it is of value for future extensions to kinematically indeterminate configurations and to geometric non-linear cases.

This work extends the original IFM [25] by adopting the product force concept from [14] in order to formulate a new force method which is here named Extended Integrated Force Method (IFME). The IFME not only inherits the advantages of the IFM over the SFM but it is also able to predict the response of prestress-stable kinematically indeterminate structures. Since the analysis of kinematically indeterminate structures is entwined with the evaluation of prestress stability, a new general formulation is included in the IFME to compute an appropriate prestress that can stabilize the structure. This formulation, which is based on semidefinite programming, is new with respect to previous works [17, 18, 19, 20] because it allows to obtain simultaneously the prestress as well as the initial element deformations that induce the required prestress. The initial element deformations are usually thought of as caused by a lack of fit and have been referred as *eigenstrain* [39]. In this work instead, prestress and corresponding *eigenstrain* are both design variables, which gives important

insights into feasibility and constructability of a prestress-stable kinematically indeterminate structure. In addition, in case the structure is equipped with an active control system, it is shown that the IFME can be used as a convenient analysis tool to model the effect of actuation in kinematically indeterminate structures including the initial actuator length changes (i.e. *eigenstrain*) to stabilize the system (Section 6).

For simplicity, only pin-jointed systems are considered. It is assumed that each structural element can take both tension and compression. In addition, the following points need to be mentioned:

- (1) The analysis is carried within the assumption of small strains and small displacements;
- (2) Mechanisms are inextensional in the sense that they are assumed to cause no first-order deformations. However, if second-order deformation occur, they are ignored due to assumption (1);
- (3) The IFME is able to compute the structural response of a prestress-stable kinematically indeterminate structural system. That is, all mechanisms shall be first-order infinitesimal mechanisms so that they can be stabilized through prestress.
- (4) Prestress stability condition is evaluated to determine whether the structure can be stabilized through prestress i.e. whether all the mechanisms are first-order infinitesimal.
- (5) For brevity, mechanisms that can be stabilized through prestress, i.e. first-order infinitesimal mechanisms, are referred as infinitesimal; higher order infinitesimal mechanisms are considered as finite.

This paper is organized as follows: Section 2 defines the main components of the IFME through the SVD decomposition of the equilibrium matrix; Section 3 gives the IFM formulation; Section 4 discusses IFM limitations with regard to analyzing prestress-stable kinematically indeterminate systems. Section 5 gives the formulation for the IFME. In section 6 examples of kinematically indeterminate structures stabilized through prestress are discussed and illustrated. Results obtained with the IFME are benchmarked against the methods based on the SFM and product force concept [35], SVD-FM [28], and DM. Section 7 and 8 conclude the paper.

2 Decomposition of the equilibrium matrix

Consider a pin-jointed structure made of n^e elements and n^n joints in d -dimensions. The rigid body motions of the system are constrained by n^c supports hence the number of free degrees of freedom is $n^f = dn^n - n^c$. The equilibrium conditions are expressed as

$$\mathbf{A}\mathbf{F} = \mathbf{P}, \quad 1$$

where $\mathbf{A} \in \mathbb{R}^{n^f \times n^e}$ is the structure equilibrium matrix containing the element direction cosines, $\mathbf{F} \in \mathbb{R}^{n^e \times 1}$ is the element force vector, and $\mathbf{P} \in \mathbb{R}^{n^f \times 1}$ is the external load vector. Denote r as the rank of the equilibrium matrix \mathbf{A} , then the number of self-stress states is $s = n^e - r$ and the number of mechanism modes is $m = n^f - r$. The equilibrium matrix \mathbf{A} can be decomposed through SVD in the following terms

$$\mathbf{A} = [\mathbf{U}_r \quad \mathbf{U}_m] \begin{bmatrix} \mathbf{V}_r & 0 \\ 0 & 0 \end{bmatrix} [\mathbf{W}_r \quad \mathbf{W}_s]^T, \quad 2$$

where $[\mathbf{U}_r \quad \mathbf{U}_m] \in \mathbb{R}^{n^f \times n^f}$, $[\mathbf{W}_r \quad \mathbf{W}_s] \in \mathbb{R}^{n^e \times n^e}$, and $\mathbf{V}_r \in \mathbb{R}^{n^f \times n^f}$ are the left singular vectors, right singular vectors and singular values of \mathbf{A} , respectively. $\mathbf{U}_r \in \mathbb{R}^{n^f \times r}$ and $\mathbf{U}_m \in \mathbb{R}^{n^f \times m}$ are the basis of the column space $\mathcal{R}(\mathbf{A}^T)$ and the left-null space $\mathcal{N}(\mathbf{A}^T)$ of the equilibrium matrix, respectively. $\mathbf{W}_r \in \mathbb{R}^{n^e \times r}$ and $\mathbf{W}_s \in \mathbb{R}^{n^e \times s}$ are the basis of the row space $\mathcal{R}(\mathbf{A})$ and the null space $\mathcal{N}(\mathbf{A})$ of the equilibrium matrix, respectively. Load components lying in the space spanned by \mathbf{U}_r can be carried by the structure in its initial configuration and they are in equilibrium with forces lying in the space spanned by $\mathbf{W}_r \in \mathbb{R}^{n^e \times r}$. The columns of \mathbf{U}_m are m linearly independent mechanism modes or in other words nodal displacements which do not cause strain (first order deformation) of the elements. Load components lying in the space spanned by \mathbf{U}_m cannot be equilibrated by the structure in its initial configuration. The columns of \mathbf{W}_s are s linearly independent self-stress states. For full static and kinematic interpretation of the terms of the SVD of the equilibrium matrix, the reader is referred to [28].

3 Integrated Force Method (IFM) formulation

The IFM combines into a single matrix statement the equilibrium equations with s extra compatibility equations

$$\mathbf{W}_s^T \mathbf{e} = \mathbf{0}, \quad 3$$

where $\mathbf{W}_s^T \in \mathbb{R}^{s \times n^e}$ is the transpose of the self-stress basis. The s compatibility conditions in Eq. 3 can be derived from virtual work or by simply considering the orthogonality between the compatible strain \mathbf{e} and the basis of incompatible strains \mathbf{w}_s (\mathbf{w}_s can be interpreted as both the self-stress and incompatible strain basis) [28]. The compatible strain \mathbf{e} can be decomposed into an elastic part $\mathbf{e}_e = \mathbf{B}\mathbf{F}$ which is caused by the force \mathbf{F} , and a non-elastic part \mathbf{e}_0 which is usually caused by lack of fit or thermal strain and it has also been referred as *eigenstrain* [39]

$$\mathbf{e} = \mathbf{B}\mathbf{F} + \mathbf{e}_0, \quad 4$$

where $\mathbf{B} \in \mathbb{R}^{n^e \times n^e}$ is the flexibility matrix which for a pin-jointed structure is a diagonal matrix whose non-zero entries are

$$B_{ii} = \frac{L_i}{E_i A_i}, \quad 5$$

and L_i , E_i , and A_i are the length, Young's modulus and cross-sectional area of element i , respectively.

Replacing \mathbf{e} in Eq. 3 through Eq. 4

$$\mathbf{W}_s^T \mathbf{B}\mathbf{F} = -\mathbf{W}_s^T \mathbf{e}_0. \quad 6$$

By concatenation of Eq. 1 and Eq. 6, the governing equation of the IFM is obtained

$$\begin{bmatrix} \mathbf{A} \\ \mathbf{W}_s^T \mathbf{B} \end{bmatrix} \mathbf{F} = \begin{bmatrix} \mathbf{P} \\ -\mathbf{W}_s^T \mathbf{e}_0 \end{bmatrix}, \quad 7$$

or in compact form

$$\mathbf{S}\mathbf{F} = \mathbf{P}^*, \quad 8$$

where

$$\mathbf{S} = \begin{bmatrix} \mathbf{A} \\ \mathbf{W}_s^T \mathbf{B} \end{bmatrix}, \quad \mathbf{P}^* = \begin{bmatrix} \mathbf{P} \\ -\mathbf{W}_s^T \mathbf{e}_0 \end{bmatrix}. \quad 9$$

In Eq. 8, $\mathbf{S} \in \mathbb{R}^{(n^f + s) \times n^e}$ and $\mathbf{P}^* \in \mathbb{R}^{(n^f + s) \times 1}$ are the governing matrix and extended load vector of the IFM, respectively. Note that \mathbf{P}^* contains the eigenstrain \mathbf{e}_0 thus allowing to set directly an initial deformation such as that caused by a lack of fit of the elements or alternatively by the length change of one or more linear actuators integrated in the structure [34].

Because $s = n^e - r$ and $m = n^f - r$ it follows that $n^f + s = n^e + m$ and thus $\mathbf{S} \in \mathbb{R}^{(n^e+m) \times n^e}$ and $\mathbf{P}^* \in \mathbb{R}^{(n^e+m) \times 1}$. For kinematically determinate systems ($m = 0$), the governing matrix $\mathbf{S} \in \mathbb{R}^{n^e \times n^e}$ is square with full rank. Under this condition, the element forces \mathbf{F} are obtained as

$$\mathbf{F} = \mathbf{S}^{-1} \mathbf{P}^* . \quad 10$$

Once the forces are known, the nodal displacements $\mathbf{U} \in \mathbb{R}^{n^f \times 1}$ are obtained as

$$\mathbf{U} = \mathbf{J}(\mathbf{B}\mathbf{F} + \mathbf{e}_0) , \quad 11$$

where

$$\mathbf{J} = \left[\mathbf{S}^{-T} \right]_{\forall i \leq n^e} , \quad 12$$

contains the first n^e rows of the transpose of the inverse of \mathbf{S} . Eq. 10 and Eq. 11 are the two key equations of the IFM to calculate the structural response under static loading for kinematically determinate systems.

4 IFM limitation for prestress-stable kinematically indeterminate systems

The IFM is able to predict the response of kinematically determinate systems ($m = 0$) efficiently and accurately [25, 30, 40]. However, problems arise if it is adopted to analyze kinematically indeterminate systems ($m > 0$).

4.1 IFM force computation limitation

A general load \mathbf{P} applied on a kinematically indeterminate system can be decomposed into two parts: the load component $\mathbf{P}^{(1)}$ lying in the column space of the equilibrium matrix that is spanned by \mathbf{U}_r ; the load component $\mathbf{P}^{(2)}$ lying in the left-null space of the equilibrium matrix that is spanned by \mathbf{U}_m . The space spanned by \mathbf{U}_r contains all the loads which can be equilibrated by the system in its initial configuration [12, 35], which means that the following equation admits at least one solution

$$\mathbf{A}\mathbf{F}^{(1)} = \mathbf{P}^{(1)} . \quad 13$$

However, the space spanned by \mathbf{U}_m contains all the loads which cannot be taken by the structure in its initial configuration due to the existence of mechanisms. This means that the following equation admits no solution when $\mathbf{P}^{(2)} \neq \mathbf{0}$

$$\mathbf{A}\mathbf{F}^{(2)} = \mathbf{P}^{(2)} . \quad 14$$

This also shows that, in general, the equilibrium equation Eq. 15 admits no solution when $\mathbf{P}^{(2)} \neq \mathbf{0}$

$$\mathbf{A}\mathbf{F} = \mathbf{P} = \mathbf{P}^{(1)} + \mathbf{P}^{(2)}. \quad 15$$

If $\mathbf{U}_m^T \mathbf{P} = \mathbf{0}$, \mathbf{P} can be equilibrated by the system in its initial configuration; if $\mathbf{U}_m^T \mathbf{P} \neq \mathbf{0}$, \mathbf{P} cannot be equilibrated by the system in its initial configuration. Therefore, when the load contains components lying in the space spanned by \mathbf{U}_m , Eq. 8 cannot be solved for forces.

4.2 IFM displacement computation limitation

Because the IFM governing matrix $\mathbf{S} \in \mathbb{R}^{(n^e+m) \times n^e}$ is not square when $m > 0$, Eq. 11 cannot be used to compute the displacements. For a kinematically indeterminate system, the displacement \mathbf{U} can be decomposed into a part \mathbf{U}_e caused by element deformations i.e. extensional displacement and a part \mathbf{U}_k due to inextensional displacements caused by infinitesimal mechanisms. That is

$$\mathbf{U} = \mathbf{U}_e + \mathbf{U}_k. \quad 16$$

The relation between \mathbf{U} and the element deformation is

$$\mathbf{A}^T \mathbf{U} = \mathbf{B}\mathbf{F} + \mathbf{e}_0. \quad 17$$

Eq. 17 can be decomposed into two equations

$$\mathbf{A}^T \mathbf{U}_e = \mathbf{B}\mathbf{F} + \mathbf{e}_0, \quad 18$$

$$\mathbf{A}^T \mathbf{U}_k = \mathbf{0}. \quad 19$$

\mathbf{U}_k can be expressed as the combination of the basis of mechanism modes \mathbf{U}_m , that is

$$\mathbf{U}_k = \mathbf{U}_m \boldsymbol{\beta}, \quad 20$$

where $\boldsymbol{\beta} \in \mathbb{R}^{m \times 1}$ is an arbitrary combination coefficient vector. For this reason, Eq. 17 admits infinite solutions.

5 Extended Integrated Force Method (IFME) formulation

5.1 Product force

The product force has been introduced in [35, 14] to compute the stiffness of first-order infinitesimal mechanisms stabilized through prestress in a kinematically indeterminate

system. Suppose element k is connected by node i and j in a pin-jointed system. For the pre-stressed configuration, the equilibrium equation in the x -direction of node i is

$$\sum_k \frac{x_i - x_j}{L_k} F_{0k} = P_{0ix}, \quad 21$$

where x_i and x_j are the coordinates in x -direction of node i and j , L_k is the length of element k , F_{0k} is the prestress in element k , and P_{0ix} is the load component in x -direction applied on node i . Then suppose that the system deforms by imposing the h^{th} inextensional displacement $\mathbf{U}_m^h \beta_h$, where β_h is a sufficiently small value to ensure the small displacement assumption holds. In the deformed configuration, second-order changes of the element lengths might occur. However, since small displacements assumption is applied, second-order deformations are neglected and thus element lengths and prestress remain unchanged. The equilibrium equation in the x -direction of node i in the deformed configuration is

$$\sum_k \frac{(x_i + U_{m,ix}^h \beta_h) - (x_j + U_{m,jx}^h \beta_h)}{L_k} F_{0k} = P_{0ix} + \delta P_{ix}^h, \quad 22$$

where δP_{ix}^h is an additional force, the so called product force or geometric load, that is required to satisfy equilibrium in the deformed configuration. Through appropriate prestress, this additional force, which arises as the mechanism is displaced, can be employed to equilibrate the external load lying in the direction of the inextensional mechanism $\mathbf{U}_m^h \beta_h$. Substituting Eq. 21 in Eq. 22 gives the product of the change of equilibrium matrix $\delta \mathbf{A}_x^h$ times the prestress and the coefficient vector β_h

$$\left(\sum_k \frac{U_{m,ix}^h - U_{m,jx}^h}{L_k} F_{0k} \right) \beta_h = \delta P_{ix}^h. \quad 23$$

Collecting Eq. 23 for all degrees of freedom gives

$$\mathbf{G}^h \beta_h = \delta \mathbf{P}^h, \quad 24$$

where

$$\mathbf{G}^h = (\delta \mathbf{A}^h) \mathbf{F}_0, \quad 25$$

and $\delta \mathbf{A}^h$ contains the change of the equilibrium matrix terms caused by the inextensional displacement of the mechanism \mathbf{U}_m^h . \mathbf{G}^h is the product force for a unit amplitude of the

mechanism \mathbf{U}_m^h and \mathbf{F}_0 is the prestress. Collecting Eq. 25 for all the mechanism modes gives the product force matrix

$$\mathbf{G} = [\mathbf{G}^1, \dots, \mathbf{G}^h, \dots, \mathbf{G}^m]. \quad 26$$

For a self-equilibrated prestress, i.e. no external load exists, \mathbf{F}_0 is expressed as a combination of the s independent self-stress states

$$\mathbf{F}_0 = \mathbf{W}_s \boldsymbol{\alpha}, \quad 27$$

where $\boldsymbol{\alpha} \in \mathbb{R}^{s \times 1}$ is the self-stress combination coefficient vector. From Eq. 25, \mathbf{G}^h in this case can be expressed as

$$\mathbf{G}^h = (\delta \mathbf{A}^h) \mathbf{W}_s \boldsymbol{\alpha}. \quad 28$$

Define $\mathbf{Q}_h = (\delta \mathbf{A}^h) \mathbf{W}_s$, then the product force matrix \mathbf{G} can be expressed as

$$\mathbf{G} = [\mathbf{Q}_h \boldsymbol{\alpha}, \dots, \mathbf{Q}_h \boldsymbol{\alpha}, \dots, \mathbf{Q}_h \boldsymbol{\alpha}] = [\mathbf{Q}_h, \dots, \mathbf{Q}_h, \dots, \mathbf{Q}_h] \boldsymbol{\Lambda}, \quad 29$$

where $\boldsymbol{\Lambda}$ is a block diagonal matrix whose diagonal entries are the self-stress combination coefficients $\boldsymbol{\alpha}$. Note that Eq. 25 and Eq. 29 are identical for a self-equilibrated prestress. Compared to Eq. 29, Eq. 25 uses the prestress \mathbf{F}_0 explicitly to express the product force instead of the self-stress states and corresponding coefficient factors .

5.2 Prestress design

The analysis of a kinematically indeterminate structures generally involves the determination of an appropriate prestress to stabilize the system. Although pre-stress stability criteria were given in [14, 15, 16], a general and efficient procedure to compute prestress that stabilizes kinematically indeterminate systems with multiple self-stress states was not addressed. In this section, a general approach that applies to systems with single and multiple self-stress states is proposed.

In order to stabilize a kinematically indeterminate system, all the mechanisms in the system should have positive stiffness. To ensure this, the scalar product of a general inextensional mechanism $\mathbf{U}_m \boldsymbol{\beta}$ and the corresponding product force vector $\mathbf{G} \boldsymbol{\beta}$ should be positive for any $\boldsymbol{\beta}$

$$\boldsymbol{\beta}^T \mathbf{G}^T \mathbf{U}_m \boldsymbol{\beta} > 0, \quad \forall \boldsymbol{\beta} \in \mathbb{R}^{m \times 1} \text{ and } \boldsymbol{\beta} \neq \mathbf{0}, \quad 30$$

which means that the matrix $\mathbf{G}^T \mathbf{U}_m$ should be positive definite [14]

$$\mathbf{G}^T \mathbf{U}_m > \mathbf{0}.$$

If Eq. 31 holds, it means that the mechanisms in the system are all first-order infinitesimal and thus the structure can be stabilized through prestress. It has been proven that for small deformations $\mathbf{G}^T \mathbf{U}_m$ is equivalent to the geometric stiffness matrix reduced to the mechanism space [36, 41] i.e. the product force could be thought of the stiffness of the mechanism.

Since prestress is obtained considering no external loads, the task is to obtain a prestress \mathbf{F}_0 which is a suitable combination of the self-stress states through the combination coefficients $\boldsymbol{\alpha}$ (Eq. 27) such that $\mathbf{G}^T \mathbf{U}_m > \mathbf{0}$. This task has been referred as ‘‘prestress design’’ in previous works [17, 18, 19]. Recently, Wang and Xu [20] formulated a prestress design process based on semi-definite programming which can be solved efficiently through a prima-dual interior algorithm. In these studies, the prestress \mathbf{F}_0 is treated as the only design variable. Instead in this work, both \mathbf{F}_0 and the *eigenstrain* \mathbf{e}_0 (initial element deformation) are treated as design variables. This allows to obtain simultaneously the prestress as well as the *eigenstrain* that induce the required prestress. In addition, in case the structure is equipped with an active control system, having both \mathbf{F}_0 and \mathbf{e}_0 as design variable, allows to obtain the initial actuator length changes (i.e. *eigenstrain*) to stabilize the system (Section 6).

Following the prestress design method proposed in [20], the process proposed here is formulated as a semi-definite programming problem (SDP)

$$\begin{aligned} \min_{\mathbf{u}, \mathbf{e}_0} \quad & -\text{Tr}(\mathbf{G}^T \mathbf{U}_m) \\ \text{s.t.} \quad & \begin{cases} \mathbf{G}^T \mathbf{U}_m - \eta \mathbf{I} \geq \mathbf{0} \\ \mathbf{W}_s^T \mathbf{B} \mathbf{F}_0 = -\mathbf{W}_s^T \mathbf{e}_0 \\ \mathbf{g}(\mathbf{F}_0, \mathbf{e}_0) \geq \mathbf{0} \\ \mathbf{F}^L \leq \mathbf{F}_0 \leq \mathbf{F}^U \\ \mathbf{e}^L \leq \mathbf{e}_0 \leq \mathbf{e}^U \end{cases} \end{aligned} \quad 32$$

where the prestress \mathbf{F}_0 and product force \mathbf{G} are expressed through Eq. 27 and Eq. 29, respectively. It is clear that since the trace of a square matrix is the sum of its eigenvalues, minimizing $-\text{Tr}(\mathbf{G}^T \mathbf{U}_m)$ is equivalent to maximizing the sum of the eigenvalues of $\mathbf{G}^T \mathbf{U}_m$, which increases the possibility to obtain a positive definite $\mathbf{G}^T \mathbf{U}_m$. In the prestress stability condition, η is a small positive value (e.g. $\eta = 0.01$) to ensure that the minimum eigenvalue of $\mathbf{G}^T \mathbf{U}_m$ is strictly positive and \mathbf{I} is an identity matrix. Since no external load is considered,

\mathbf{F}_0 and \mathbf{e}_0 are related directly through the compatibility conditions expressed in Eq. 6. A general linear function $\mathbf{g}(\mathbf{F}_0, \mathbf{e}_0) \geq \mathbf{0}$ is introduced to constrain prestress and *eigenstrain*. For example, if prestress and initial deformations of elements i and j are required to be identical, then the linear constraints are $\mathbf{F}_{0,i} = \mathbf{F}_{0,j}$ and $\mathbf{e}_{0,i} = \mathbf{e}_{0,j}$. Lower and upper bounds for \mathbf{F}_0 and \mathbf{e}_0 are denoted as $\mathbf{F}^L, \mathbf{e}^L$ and $\mathbf{F}^U, \mathbf{e}^U$, respectively, which can be set to account for stress and length change limits. In case prestress is introduced through active control, the bounds on \mathbf{e}_0 allow to constrain the actuator length changes to induce the prestress \mathbf{F}_0 .

Eq. 32 is a SDP model which can be solved globally through a primal-dual interior-point algorithm [42]. Note that besides the objective function adopted here, other objectives can also be employed according to requirements as long as they can be formulated into linear forms with respect to the optimization variables \mathbf{F}_0 and \mathbf{e}_0 . Since the SDP model is convex, if Eq. 32 admits a solution, it is the global optimum and hence it means that the structure can be stabilized through prestress subject to the considered constraints. If Eq. 32 is infeasible, it means that the structure cannot be stabilized through prestress subject to the considered constraints.

The problem stated in Eq. 32 is a general prestress design model that applies to kinematically indeterminate structures with single and multiple self-stress states. However, note that Eq. 32 is a numerical optimization model in which some specific constraints on prestress \mathbf{F}_0 and initial deformation \mathbf{e}_0 are considered. In addition, a small positive value must be set for η to ensure that the minimum eigenvalue of $\mathbf{G}^T \mathbf{U}_m$ is strictly positive. Therefore, infeasibility of Eq. 32 might not necessarily mean that the system cannot be stabilized by any prestress, i.e. it indicates that there is no prestress that satisfies the assigned constraints within the set tolerance η for the positive definiteness of $\mathbf{G}^T \mathbf{U}_m$. That being said, if no constraints on \mathbf{F}_0 and \mathbf{e}_0 are assigned and η is set to a sufficiently small value, if there is no solution to Eq. 32, the system can be practically referred to as ‘not prestress-stable’.

5.3 IFME governing equation and computation of forces

A prestress-stable kinematically indeterminate system has two different modes to equilibrate an external load: (1) element deformations produce forces that equilibrate the load; and (2) inextensional displacements at constant prestress, in which case the load is equilibrated by out-of-balance forces arising from the reorientation of the elements i.e. a change of geometry

[43, 35]. This out-of-balance force is the product force as defined in Section 5.1. The product force can also be thought of as the stiffness of the mechanism [36]. Load components $\mathbf{P}^{(1)}$ lying in the column space of the equilibrium matrix that is spanned by \mathbf{U}_r are equilibrated through the first mode. Load components $\mathbf{P}^{(2)}$ lying in the left-null space of the equilibrium matrix that is spanned by \mathbf{U}_m can be equilibrated through the second mode (i.e. through prestress).

The equilibrium conditions for the first mode are given directly through the equilibrium matrix \mathbf{A} (Eq. 1). Recalling Eq. 24, the equilibrium conditions for the second mode are expressed as

$$\mathbf{G}\boldsymbol{\beta} = \mathbf{P}^{(2)}, \quad 33$$

where $\mathbf{G} \in \mathbb{R}^{n^f \times m}$ is the product force matrix and $\boldsymbol{\beta} \in \mathbb{R}^{m \times 1}$ is the combination coefficient vector of the mechanism modes.

In order to extend the IFM to the analysis of prestress-stable kinematically indeterminate systems, the equilibrium conditions for the second mode are incorporated by combining Eq. 1 and Eq. 33

$$\mathbf{A}\mathbf{F}^{(1)} + \mathbf{G}\boldsymbol{\beta} = \mathbf{P}^{(1)} + \mathbf{P}^{(2)}. \quad 34$$

By combining the equilibrium condition Eq. 34 and compatibility condition Eq. 6, a new governing equation is obtained

$$\begin{bmatrix} \mathbf{A} & \mathbf{G} \\ \mathbf{W}_s^T \mathbf{B} & \mathbf{0} \end{bmatrix} \begin{bmatrix} \mathbf{F} \\ \boldsymbol{\beta} \end{bmatrix} = \begin{bmatrix} \mathbf{P} \\ -\mathbf{W}_s^T \mathbf{e}_0 \end{bmatrix}, \quad 35$$

or

$$\mathbf{S}^* \mathbf{F}^* = \mathbf{P}^*, \quad 36$$

where

$$\mathbf{S}^* = \begin{bmatrix} \mathbf{A} & \mathbf{G} \\ \mathbf{W}_s^T \mathbf{B} & \mathbf{0} \end{bmatrix}, \quad \mathbf{F}^* = \begin{bmatrix} \mathbf{F} \\ \boldsymbol{\beta} \end{bmatrix}. \quad 37$$

In Eq. 36, $\mathbf{S}^* \in \mathbb{R}^{(n^e+m) \times (n^e+m)}$ is the IFME governing matrix, and $\mathbf{F}^* \in \mathbb{R}^{(n^e+m) \times 1}$ is a vector containing the unknown force \mathbf{F} and the coefficient vector $\boldsymbol{\beta}$. For a prestress-stable kinematically indeterminate structure, the m mechanisms are first-order infinitesimal and thus

they gain positive stiffness through prestress \mathbf{F}_0 . The union of the equilibrium matrix \mathbf{A} and product force matrix \mathbf{G} , i.e. $[\mathbf{A} \parallel \mathbf{G}]$, spans $\mathcal{R}(\mathbf{A}^T) \oplus \mathcal{N}(\mathbf{A}^T)$ (which is referred as the joint space in [35]), and therefore $[\mathbf{A} \parallel \mathbf{G}]$ has full row rank. By integrating the compatibility equations in Eq. 6, the governing matrix \mathbf{S}^* is full-rank and thus it can be inverted. Solving Eq. 37 for \mathbf{F}^*

$$\mathbf{F}^* = [\mathbf{S}^*]^{-1} \mathbf{P}^*. \quad 38$$

The IFME governing equation allows to compute the structural response of statically and kinematically indeterminate systems subject to any arbitrary load including those that have components lying in the left-null space of the equilibrium matrix, i.e. loads that without appropriate prestress cause instability due to first-order infinitesimal mechanisms.

5.4 IFME compatibility conditions and computation of displacements

Eq. 38 yields, besides the element forces \mathbf{F} , also the combination coefficient vector of the mechanism modes $\boldsymbol{\beta}$ and thus the inextensional displacement \mathbf{U}_k can be calculated through Eq. 20. Using virtual work, it is possible to prove the orthogonality between the product force \mathbf{G} and the extensional displacement \mathbf{U}_e [35]. Suppose a system in its initial configuration, the external load and element force are denoted by \mathbf{P} and \mathbf{F} , respectively; the extensional displacements \mathbf{U}_e are compatible with the element elongations $\delta \mathbf{e}$. Then, from virtual work

$$\mathbf{P}^T \mathbf{U}_e = \mathbf{F}^T \delta \mathbf{e}. \quad 39$$

Suppose that the system deforms by imposing an inextensional displacement $\mathbf{U}_m \boldsymbol{\beta}$, where $\boldsymbol{\beta}$ is sufficiently small to ensure that small displacement assumption holds. The inextensional displacement does not cause first order element deformations (hence within the small strains assumption it does not cause a change of the element forces) but will produce out of balance forces i.e. the product force $\mathbf{G} \boldsymbol{\beta}$. Therefore, applying virtual work

$$(\mathbf{P} + \mathbf{G} \boldsymbol{\beta})^T (\mathbf{U}_e + \mathbf{U}_m \boldsymbol{\beta}) = \mathbf{F}^T \delta \mathbf{e}. \quad 40$$

Expanding Eq. 40 gives

$$\mathbf{P}^T \mathbf{U}_e + \mathbf{P}^T (\mathbf{U}_m \boldsymbol{\beta}) + (\mathbf{G} \boldsymbol{\beta})^T \mathbf{U}_e + (\mathbf{G} \boldsymbol{\beta})^T (\mathbf{U}_m \boldsymbol{\beta}) = \mathbf{F}^T \delta \mathbf{e}. \quad 41$$

Considering $\mathbf{U}_m^T \mathbf{P} = \mathbf{0}$ and ignoring the higher-order term $(\mathbf{G} \boldsymbol{\beta})^T (\mathbf{U}_m \boldsymbol{\beta})$, Eq. 41 becomes

$$\mathbf{P}^T \mathbf{U}_e + (\mathbf{G}\boldsymbol{\beta})^T \mathbf{U}_e = \mathbf{F}^T \delta \mathbf{e}, \quad 42$$

or

$$\mathbf{P}^T \mathbf{U}_e + \boldsymbol{\beta}^T \mathbf{G}^T \mathbf{U}_e = \mathbf{F}^T \delta \mathbf{e}. \quad 43$$

Recalling Eq. 39 it follows that

$$\boldsymbol{\beta}^T \mathbf{G}^T \mathbf{U}_e = 0. \quad 44$$

Since $\boldsymbol{\beta}$ can take any values, Eq. 44 is equivalent to

$$\mathbf{G}^T \mathbf{U}_e = \mathbf{0}, \quad 45$$

which proves the orthogonality between the product force \mathbf{G} and the extensional displacement \mathbf{U}_e .

By combining Eq. 18 and Eq. 45, an extended compatibility equation is obtained

$$\begin{bmatrix} \mathbf{A}^T \\ \mathbf{G}^T \end{bmatrix} \mathbf{U}_e = \begin{bmatrix} \mathbf{B}\mathbf{F} + \mathbf{e}_0 \\ \mathbf{0} \end{bmatrix}, \quad 46$$

or

$$\mathbf{H}\mathbf{U}_e = \mathbf{E}, \quad 47$$

where

$$\mathbf{H} = \begin{bmatrix} \mathbf{A}^T \\ \mathbf{G}^T \end{bmatrix}, \mathbf{E} = \begin{bmatrix} \mathbf{B}\mathbf{F} + \mathbf{e}_0 \\ \mathbf{0} \end{bmatrix}. \quad 48$$

In Eq. 47, $\mathbf{H} \in \mathbb{R}^{(n^e+m) \times n^f}$ is the IFME compatibility matrix. For a prestress-stable kinematically indeterminate system, a unique extensional displacement can be determined

through Eq. 47. As explained in Section 5.3, $[\mathbf{A} \mid \mathbf{G}]$ has full row rank, thus $[\mathbf{A} \mid \mathbf{G}]^T = \begin{bmatrix} \mathbf{A}^T \\ \mathbf{G}^T \end{bmatrix}$

has full column rank. Accordingly, \mathbf{U}_e can be computed as

$$\mathbf{U}_e = \mathbf{H}^+ \mathbf{E}, \quad 49$$

where \mathbf{H}^+ is the Moore-Penrose pseudoinverse [44] of matrix \mathbf{H} . Finally, the total displacement \mathbf{U} (Eq. 16) can be calculated by adding the inextensional displacement

$$\mathbf{U} = \mathbf{H}^+ \mathbf{E} + \mathbf{U}_m \boldsymbol{\beta}, \quad 50$$

where $\boldsymbol{\beta}$ is the combination coefficient vector of the mechanism modes obtained from Eq. 38.

In addition to using Eq. 49, the transpose of the governing matrix \mathbf{S}^* can be utilized directly to calculate the extensional displacement \mathbf{U}_e

$$\mathbf{C}^* \mathbf{U}'_e = \mathbf{E}, \quad 51$$

where $\mathbf{C}^* \in \mathbb{R}^{(n^e+m) \times (n^e+m)}$ and $\mathbf{U}'_e \in \mathbb{R}^{(n^f+s) \times 1}$ are defined as

$$\mathbf{C}^* = [\mathbf{S}^*]^\top, \quad \mathbf{U}'_e = \begin{bmatrix} \mathbf{U}_e \\ \mathbf{0}_{s \times 1} \end{bmatrix}. \quad 52$$

Because \mathbf{S}^* is full-rank, \mathbf{U}'_e can be calculated directly by

$$\mathbf{U}'_e = [\mathbf{C}^*]^{-1} \mathbf{E} = [\mathbf{S}^*]^{-\top} \mathbf{E}, \quad 53$$

then \mathbf{U}_e can be obtained by extracting the first n^f entries of \mathbf{U}'_e and the total displacement can be computed as:

$$\mathbf{U} = \left\{ [\mathbf{C}^*]^{-1} \mathbf{E} \right\}_{\forall i \leq n^f} + \mathbf{U}_m \boldsymbol{\beta}, \quad 54$$

Eq. 49 and Eq. 53 are equivalent to compute the extensional displacement \mathbf{U}_e and Eq. 50 and Eq. 54 are equivalent to compute the total displacement \mathbf{U} . Eq. 49 is a reduced version of Eq. 53 and \mathbf{H} is a reduced version of the full IFME compatibility matrix $\mathbf{C}^* = [\mathbf{S}^*]^\top$. Similar to the SFM, the static-kinematic duality between \mathbf{S}^* and \mathbf{C}^* holds.

5.5 IFME analysis process

The IFME analysis process is summarized in the block diagram shown in Figure 1.

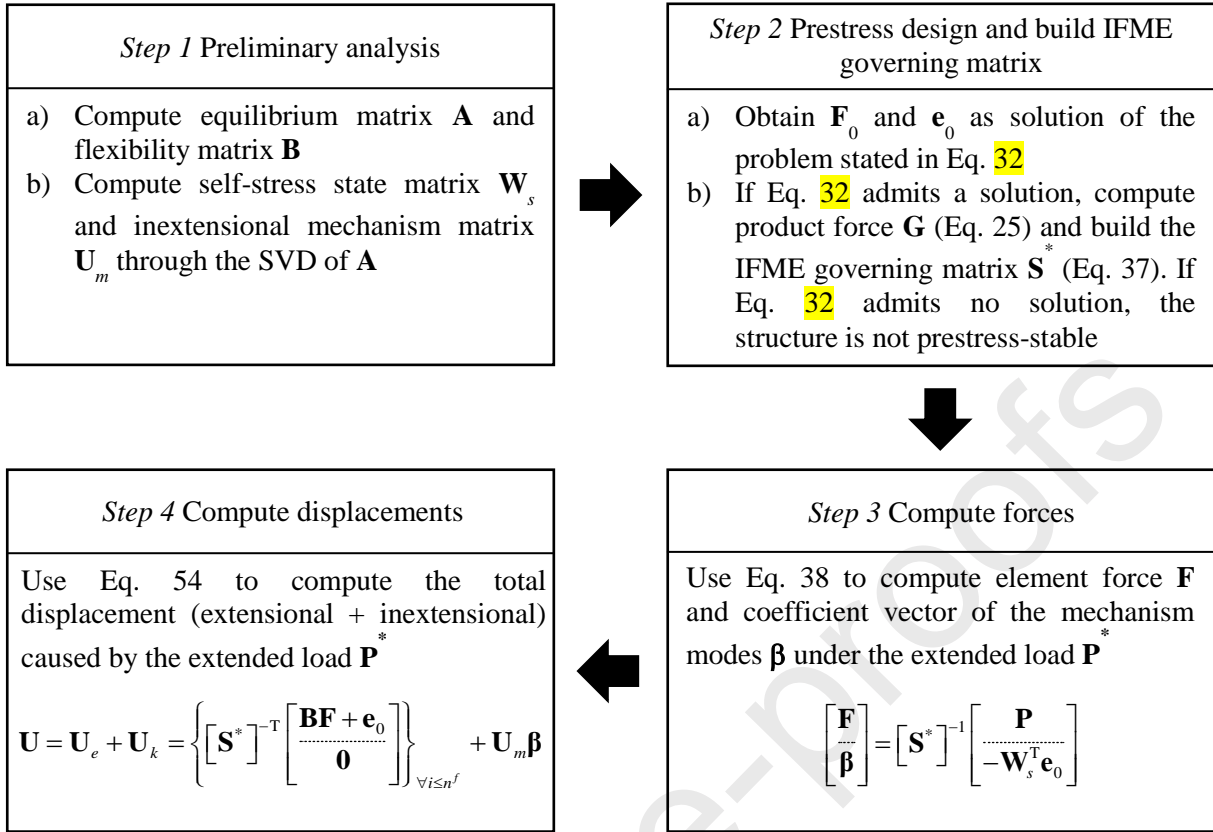


Figure 1 IFME analysis process

Note that when the extended load vector includes the *eigenstrain* \mathbf{e}_0 , the element forces obtained through Eq. 38 include the prestress \mathbf{F}_0 and the forces \mathbf{F}_{load} caused by the external load \mathbf{P} i.e. $\mathbf{F} = \mathbf{F}_0 + \mathbf{F}_{load}$. Similarly, when \mathbf{e}_0 is included in Eq. 54 the displacement \mathbf{U} includes the initial displacement \mathbf{U}_0 caused by \mathbf{e}_0 and the displacement $\mathbf{U}_{load} = \mathbf{U}_e + \mathbf{U}_k$ caused by the external load \mathbf{P} , and therefore the total displacement is $\mathbf{U} = \mathbf{U}_0 + \mathbf{U}_{load}$.

5.6 On the relation between *eigenstrain* \mathbf{e}_0 and prestress \mathbf{F}_0

As explained in 3, the *eigenstrain* \mathbf{e}_0 can be employed to model the effect of a non-elastic deformation of the elements such as that caused by thermal strains, a lack of fit or alternatively by the length change of one or more linear actuators integrated in the structure [34]. For this reason, the *eigenstrain* \mathbf{e}_0 can be also employed to cause prestress \mathbf{F}_0 through an initial non-elastic element deformation which involves a change of geometry from the initial configuration. For example, assume that \mathbf{L} are the element lengths in the intended geometry before construction. Through \mathbf{e}_0 it is possible to obtain the initial element lengths $\mathbf{L}_0 = \mathbf{L} + \mathbf{e}_0$ so that after assembling, prestress \mathbf{F}_0 will arise due to a lack of fit. Note that in this case the geometry after assembling will be different to the intended geometry. This is particularly

useful when the prestress is caused by an active system which is integrated into the structure. In this case, prestress \mathbf{F}_0 is caused directly through elongation and/or shortening (*eigenstrain* \mathbf{e}_0) of linear actuators integrated into the structure, as it will be shown in Example 4.

However, if the initial geometry is intended to remain unchanged after the application of prestress \mathbf{F}_0 , the initial element lengths must be assigned differently. For example, suppose the required length of the i^{th} element in the intended geometry is L_i , then the initial length $L_{0,i}$ and prestress $F_{0,i}$ of the i^{th} element are related by

$$\frac{E_i A_i}{L_i} (L_i - L_{0,i}) = F_{0,i}, \quad 55$$

which gives

$$L_{0,i} = \frac{E_i A_i L_i}{F_{0,i} + E_i A_i}. \quad 56$$

Pre-elongation and/or pre-shortening is introduced in the elements before assembling in order to obtain the required prestress as well as a prescribed geometry through an initial elastic deformation of the elements. Note that it is assumed the node positions can be held fixed by a rigid falsework so that during assembling the geometry of the structure remains unchanged. In this case, Eq. 38 and 54 should be used to obtain forces \mathbf{F}_{load} and displacement \mathbf{U}_{load} caused by the external load \mathbf{P} only as the eigenstrain \mathbf{e}_0 is not included. The total force in the elements will still be $\mathbf{F} = \mathbf{F}_0 + \mathbf{F}_{load}$ but the total displacement only includes the contribution of the external load i.e. $\mathbf{U} = \mathbf{U}_{load}$.

6 Numerical examples

6.1 Example 1

Consider a two-dimensional pin-jointed system consisting of two elements and three nodes shown in Figure 2(a). A vertical load P is applied at node #2. The system has one state of self-stress and one mechanism mode which is the vertical movement of node #2 as indicated by dashed lines in Figure 2(b). To benchmark the solution produced by the IFME against the analytical solution, loading and element characteristics are identical to those reported in [45]. Assume $L = 5080$ mm, $P = 311.38$ N, and $EA = 564.92$ N for the two elements.

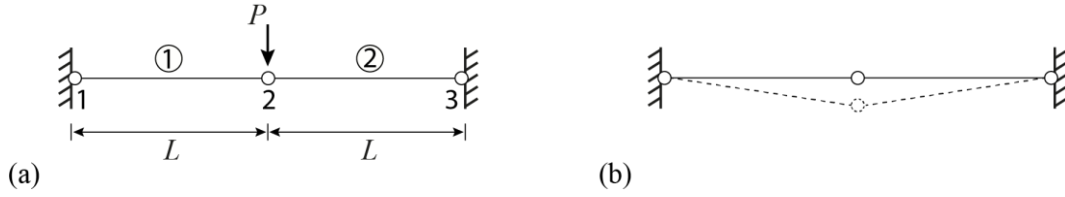


Figure 2 Example 1, planar pin-jointed system: (a) dimensions and loading, (b) internal mechanism mode

S1) Preliminary analysis

The equilibrium matrix \mathbf{A} , flexibility matrix \mathbf{B} , states of self-stress matrix \mathbf{W}_s and mechanism matrix \mathbf{U}_m are

$$\mathbf{A} = \begin{bmatrix} 1 & -1 \\ 0 & 0 \end{bmatrix}, \mathbf{B} = \begin{bmatrix} 8.9924 & 0 \\ 0 & 8.9924 \end{bmatrix}, \mathbf{W}_s = \begin{bmatrix} 1 \\ 1 \end{bmatrix}, \mathbf{U}_m = \begin{bmatrix} 0 \\ 1 \end{bmatrix}, \mathbf{P} = \begin{bmatrix} 0 \\ 1 \end{bmatrix}. \quad 57$$

Because $\mathbf{U}_m^T \mathbf{P} \neq 0$, the load \mathbf{P} contains component that lies in the left-null space of the equilibrium matrix, i.e. load \mathbf{P} cannot be equilibrated by the structure in its initial configuration.

S2) Assign prestress and compute IFME governing matrix

Suppose that a prestress tension $F_0 = 4448.2$ N is applied for both elements as done in [45]. A further check through Eq. 31 indicates that this prestress can stabilize the mechanism. Use prestress \mathbf{F}_0 to construct the product force matrix \mathbf{G} and the governing matrix \mathbf{S}^*

$$\mathbf{G} = \begin{bmatrix} 0 \\ 1.7513 \end{bmatrix}, \mathbf{S}^* = \begin{bmatrix} 1 & -1 & 0 \\ 0 & 0 & 1.7513 \\ 8.9924 & 8.9924 & 0 \end{bmatrix}. \quad 58$$

S3) Compute forces

Use Eq. 38 to obtain \mathbf{F}^*

$$\mathbf{F}^* = \begin{bmatrix} 0 \\ 0 \\ -177.80 \end{bmatrix}, \quad 59$$

or

$$\mathbf{F} = \begin{bmatrix} 0 \\ 0 \end{bmatrix}, \boldsymbol{\beta} = [-177.80]. \quad 60$$

The external load \mathbf{P} does not change the element forces but it excites the mechanism mode.

S4) Compute displacements

Use Eq. 54 to obtain the total (extensional \mathbf{U}_e + inextensional \mathbf{U}_k) displacement

$$\mathbf{U} = \mathbf{U}_e + \mathbf{U}_k = \begin{bmatrix} 0 \\ 0 \end{bmatrix} + \begin{bmatrix} 0 \\ -177.80 \end{bmatrix} = \begin{bmatrix} 0 \\ -177.80 \end{bmatrix}. \quad 61$$

No element forces are caused by the external load, i.e. the element elastic strain is zero and thus the extensional nodal displacement is zero. This is consistent with the forces obtained from Eq. 60.

Results obtained through the IFME are practically identical with those obtained by using the methods based on SFM [35] and DM [36]. However, the SVD-FM is not applicable to this system. In fact, the nodal displacement obtained through the SVD-FM is a zero vector. This is because the SVD-FM does not account for the change of stiffness of the mechanism through prestress; thus it cannot give a correct solution in terms of nodal displacements if the load contains components that lies in the left-null space of the equilibrium matrix.

According to the analytical solution given in [45] the vertical displacement of node #2 is -166.54 mm. The same system has been studied in [46] through geometric nonlinear analysis, which shows a very good accordance with the analytical solution. The error of the IFME solution with respect to the analytical solution is 6.7%. This is because in the IFME, the element lengths are assumed to remain unchanged by the first-order infinitesimal displacement. If second order element deformations caused by the inextensional displacement are considered, additional forces are developed, which subsequently increase the stiffness of the mechanism thus reducing the vertical displacement of node #2. Future work could look into an extension of the IFME to geometric non-linear cases.

6.2 Example 2

Figure 3(a) shows another example of a two-dimensional pin-jointed system which has one state of self-stress and one mechanism mode. The motion caused by the mechanism is indicated by dashed lines in Figure 3(b). Assume $L = 1.0$, $P_1 = P_2 = P_3 = 1$, $P_4 = 2$, and $EA = 1.0 \times 10^6$ for all the elements. No initial strain or prestress is applied. This system was investigated in [28] using the SVD-FM. In this case, it is possible to use the SVD-FM because the external load does not excite the mechanism. The load in fact lies in the column space of the equilibrium matrix. For this reason, it is not necessary to consider the product

force. The response obtained through the IFME is given in Table 1, which is identical to that obtained through the SVD-FM.

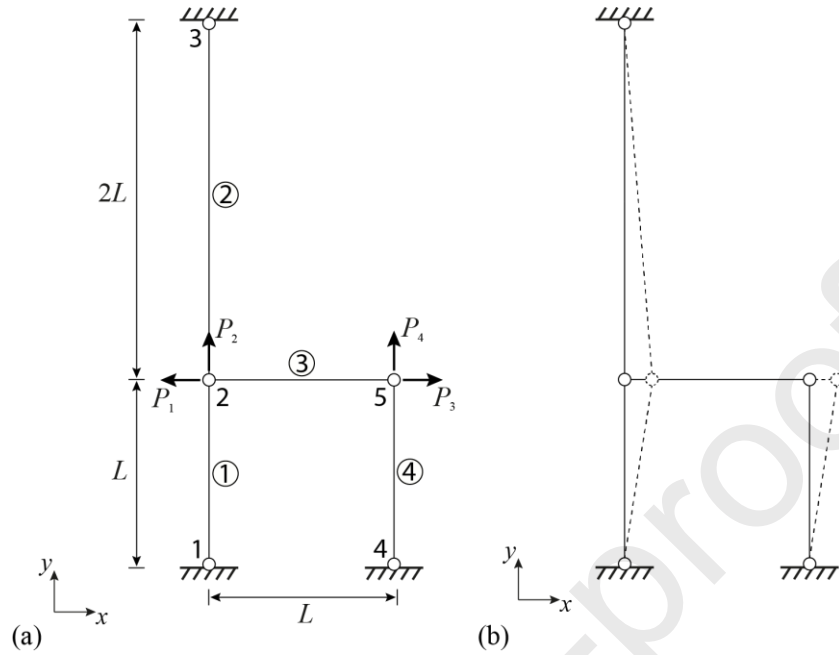


Figure 3 Example 2, planar pin-jointed system: (a) dimensions and loading, (b) internal mechanism mode

Table 1 Element force (\mathbf{F}_{load}) and nodal displacement (\mathbf{U}_{load}) caused by external load

Element Forces				Nodal Displacements ($\times 10^{-4}$)			
1	2	3	4	2-x	4-x	2-y	4-y
0.667	-0.333	1.000	2.000	-0.800	0.200	0.667	2.000

Suppose that an additional load $\Delta P = 0.1$ is applied on node #5 in the x -direction. The element forces in Table 1, which are caused by the load applied in the first phase, can be thought of as prestress to construct the product force matrix. The additional element forces and nodal displacements (Table 2), caused by ΔP are computed following the IFME analysis process outlined in Section 5.5.

Table 2 Element force ($\Delta \mathbf{F}$) and nodal displacement ($\Delta \mathbf{U}$) caused by ΔP

Element Forces				Nodal Displacements			
1	2	3	4	2-x	4-x	2-y	4-y
0.000	0.000	0.020	0.000	0.040	0.040	0.000	0.000

The final element forces and nodal displacements are obtained by summing the results in Table 1 and Table 2. A benchmark with the results obtained through the methods based on

the SFM [35] and DM [36] shows they are practically identical with those obtained through the IFME. However, similar to Example 1, the SVD-FM cannot deal with the additional load ΔP because this lies in the left-null space of the equilibrium matrix. The solution of the second step obtained through the SVD-FM is given in Table 3. Both element forces and nodal displacements are different to those given in Table 2.

Table 3 Element force (ΔF^{SVD-FM}) and nodal displacement (ΔU^{SVD-FM}) compute through SVD-FM

Element Forces				Nodal Displacements ($\times 10^{-6}$)			
1	2	3	4	2-x	4-x	2-y	4-y
0.000	0.000	0.050	0.000	-0.040	0.010	0.000	0.000

6.3 Example 3

The triplex tensegrity tower shown in Figure 4 is considered in this example. The structure is made of three identical simplex tensegrity modules one of which is shown in Figure 4(a). The structure consists of 12 nodes and 30 elements. The nodal coordinates are given in Table 4. Node #1 is fully constrained, node #2 is allowed to move in the x -direction, node #3 is allowed to move in the x - y plane, and all the other nodes are free. Considering the symmetry of the configuration, the elements are divided into six groups (Table 5). Elements in group 1 to group 4 are required to be in tension while elements in group 5 and group 6 in compression. The elements in tension have a circular section (diameter = 10.8 mm) with an area $A = 91.61 \text{ mm}^2$. The elements in compression have a circular hollow section (diameter = 60 mm, thickness = 3 mm) with an area $A = 537.21 \text{ mm}^2$, second moment of area $I = 2.19 \times 10^5 \text{ mm}^4$. The Young's modulus for the elements in compression and tension are $E = 206 \text{ GPa}$ and $E = 185 \text{ GPa}$, respectively. The stress limit for members in tension and compression are reached for a force of 115.43 kN and 166.54 kN, respectively. The Euler buckling limit for the members in compression is 230.14 kN. The displacement limit is set to $U_{\text{limit}} = 10 \text{ mm}$.

Three loads in the negative z -direction with the same magnitude $P = 1 \text{ kN}$ are applied to node #10, node #11, and node #12, respectively as shown in Figure 4(c). Preliminary analysis (Step 1) indicates that this structure has three mechanism modes (Figure 5) and three independent self-stress states. The product $U_m^T \mathbf{P} \neq \mathbf{0}$ indicates that the external load \mathbf{P} contains components lying in the left-null space of the equilibrium matrix.

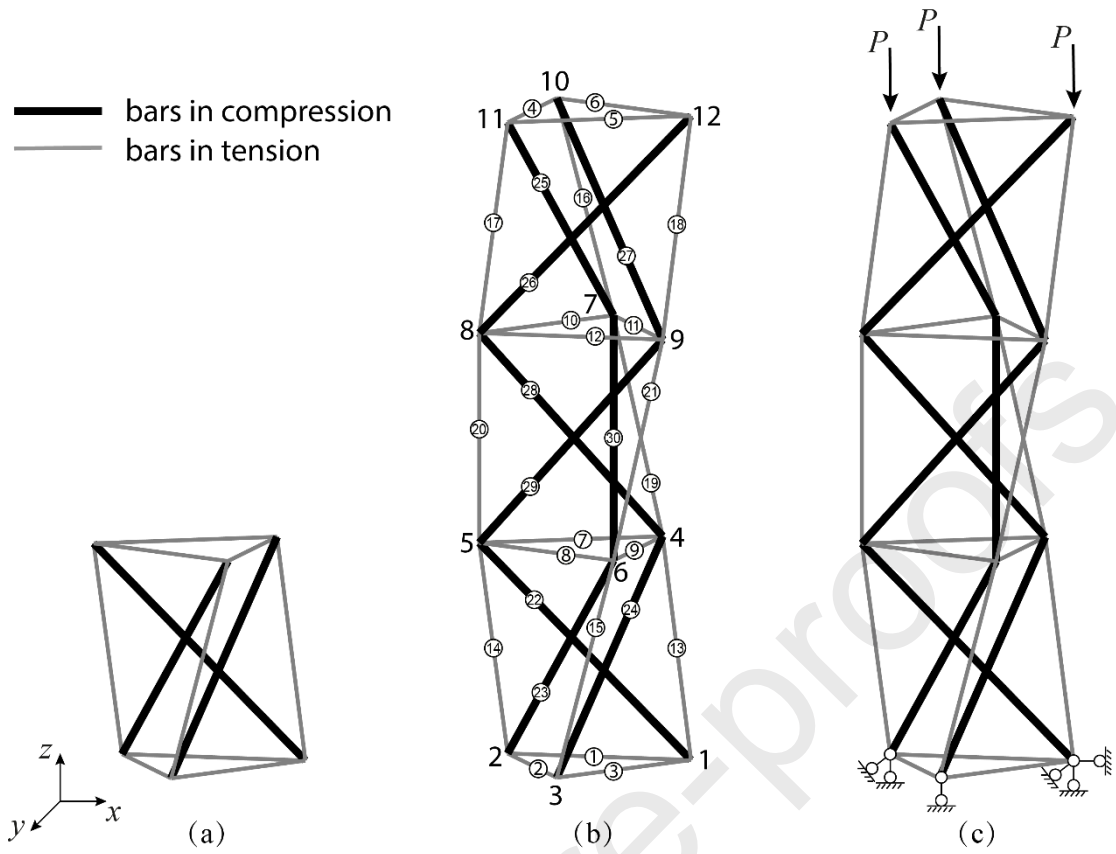


Figure 4 Triplex tensegrity tower: (a) basic simplex tensegrity module; (b) node and element numbers; and (c) supports and loading

Table 4 Triplex tensegrity tower nodal coordinates (unit mm)

Node number	X	Y	Z
1	500	0	0
2	-250	433	0
3	-250	-433	0
4	433	250	1000
5	-433	250	1000
6	0	-500	1000
7	250	433	2000
8	-500	200	2000
9	250	-433	2000
10	0	500	3000
11	-433	-250	3000
12	433	-250	3000

Table 5 Triplex tensegrity tower element groups

Element group	1	2	3	4	5	6
Element number	1-6	7-12	13-18	19-21	22-27	28-30

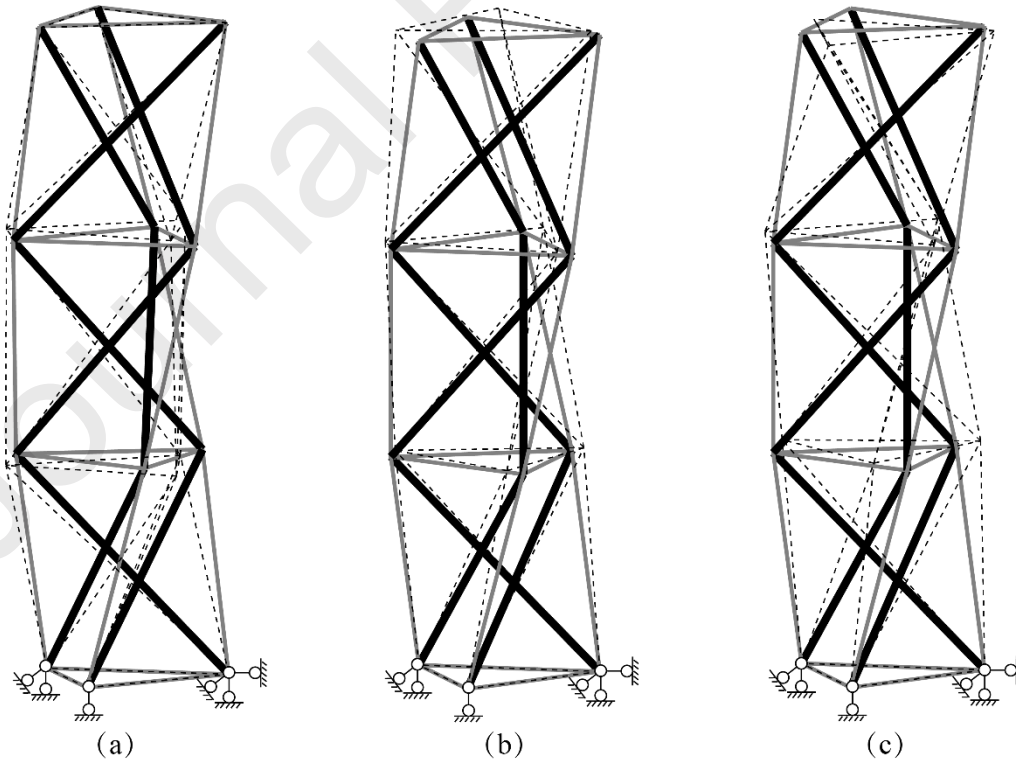


Figure 5 Mechanism modes (dashed line) of the triplex tensegrity tower

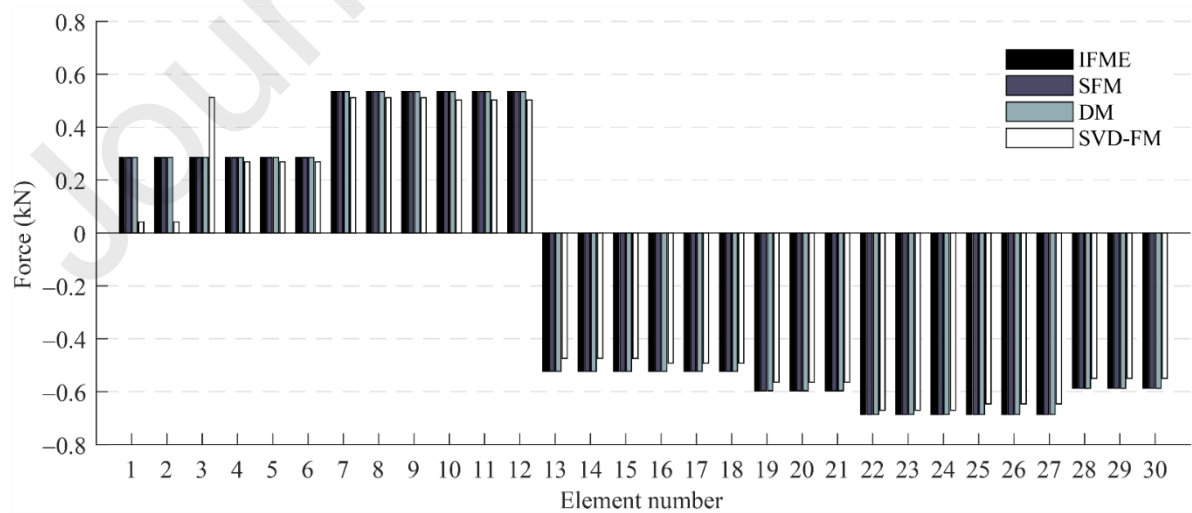
The prestress F_0 and corresponding *eigenstrain* e_0 are calculated through solving the problem stated in Eq. 32 (Step 2). Elements in the same group are constrained to have identical prestress and *eigenstrain*. Upper bounds on the absolute values of F_0 and e_0 are set to 100 kN and 5 mm, respectively. The problem stated in Eq. 32 admits a solution which is given in Table 6, hence the structure is prestress-stable.

Table 6 Prestress and *eigenstrain*

Element group	1	2	3	4	5	6
Prestress (kN)	35.962	71.925	74.296	74.296	-100.000	-100.000
<i>Eigenstrain</i> (mm)	-1.232	-3.215	-2.397	-2.364	3.223	3.195

The prestress F_0 (Table 6) and related product force G allow to build the IFME governing matrix S^* . Element forces (Step 3) and nodal displacement (Step 4) are computed following the IFME analysis process outlined in Section 5.5.

Results obtained through IFME are benchmarked with those from SFM, DM, and SVD-FM. Figure 6 show the bar chart of element forces F_{load} and nodal displacements U_{load} caused by external load P , which are computed through Eq. 38 and Eq. 54 without including e_0 . Results produced by IFME are practically identical to those produced by the SFM and DM. However, results obtained through SVD-FM are different especially in terms of displacements which are much smaller (they are barely visible in Figure 6 (b)) compared to those produced by the other methods. This is because the SVD-FM cannot consider the inextensional displacements excited by the external load which in this case are dominant.

(a) Force F_{load} caused by external load P

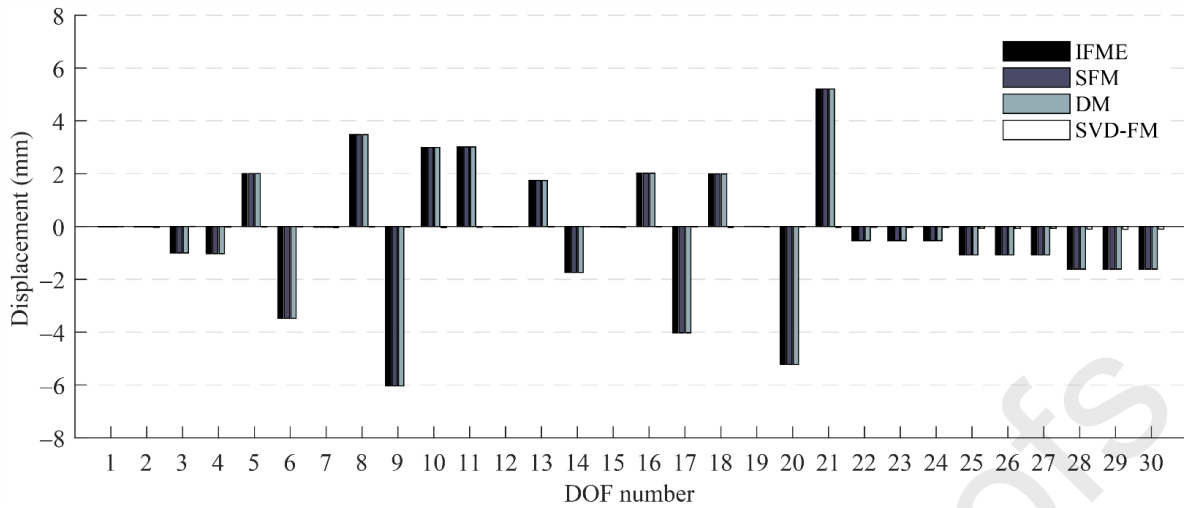
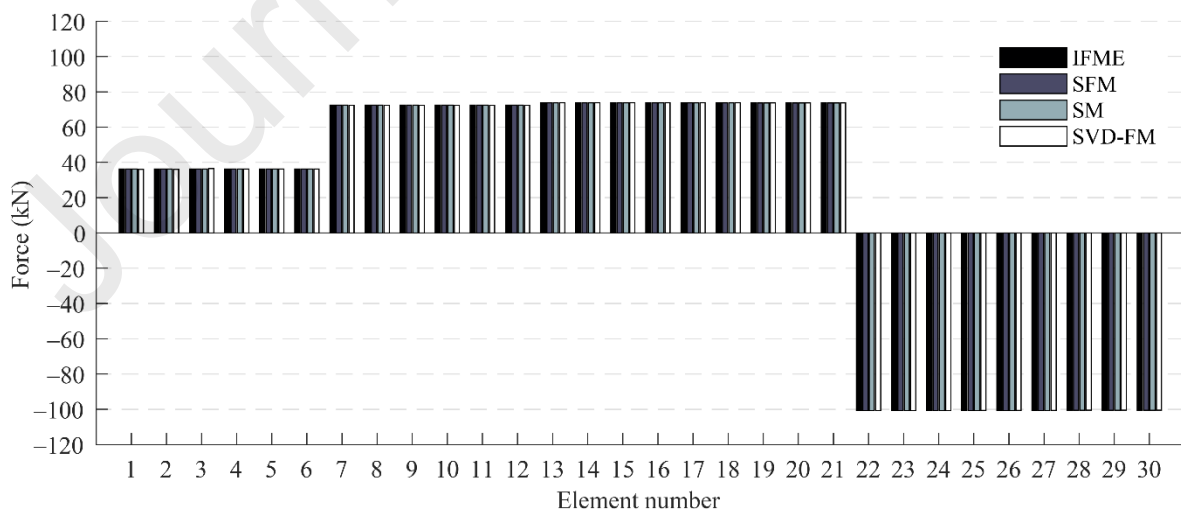
(b) Displacement \mathbf{U}_{load} caused by external load \mathbf{P}

Figure 6 Forces and displacements caused by external load obtained through IFME, SFM, DM, and SVD-FM

Figure 7 shows the bar charts of the total force $\mathbf{F} = \mathbf{F}_0 + \mathbf{F}_{load}$ and the total displacement $\mathbf{U} = \mathbf{U}_0 + \mathbf{U}_{load}$, where \mathbf{U}_0 is the initial nodal displacement caused by \mathbf{e}_0 . Referring to the result produced by the IFME, all element forces are within required limits for the admissible stress and buckling and the maximum displacement is lower than the required limit. Prestress and initial displacement are identical for all methods, thus the results produced by the SVD-FM differ primarily because of the contribution of the external load. The total forces obtained through SVD-FM are similar to those obtained through the other methods because prestress is dominant. However, the total displacements are significantly different to those obtained through the other methods because the SVD-FM cannot account for the inextensional displacements excited by the external load.

(a) Total force $\mathbf{F} = \mathbf{F}_0 + \mathbf{F}_{load}$

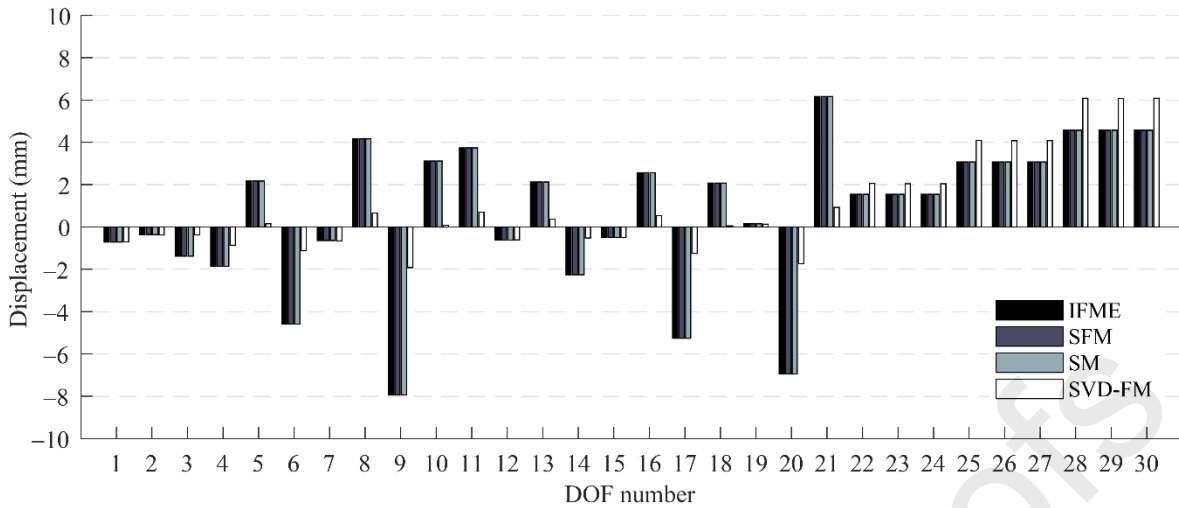
(b) Total displacement $\mathbf{U} = \mathbf{U}_0 + \mathbf{U}_{load}$

Figure 7 Total forces and displacements obtained through IFME, SFM, DM, and SVD-FM

6.4 Example 4

Consider the pin-jointed structure shown in Figure 8. All the nodes and elements lie in the x - y plane. Node #1 is fully constrained, node #2 is allowed to move in the x -direction, node #4 is allowed to move in the x - y plane, and node #3 is free. This structure is a class-1 tensegrity (at most one element under compression connecting to each joint) [47].

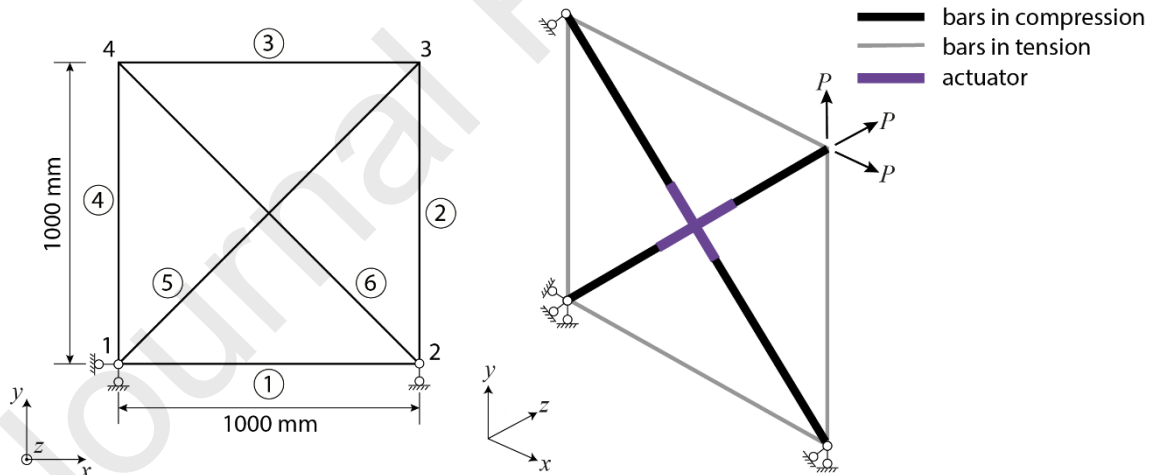


Figure 8: Pin-jointed structure consisting of four nodes and six elements.

The bars in tension (i.e. the two bracing elements) and compression (i.e. the four external elements) are assumed to have the same cross-sections and material properties as those in Example 3. The two bracing elements are equipped with linear actuators which are employed to change length in order to control element forces and nodal displacements. Three loads in x ,

y, and z-direction respectively with the same magnitude $P = 1$ kN are applied to node #3. The displacement limit is set to $U_{\text{limit}} = 10$ mm.

The product $\mathbf{U}_m^T \mathbf{P} \neq \mathbf{0}$ indicates that the external load \mathbf{P} contains components lying in the left-null space of the equilibrium matrix. This structure has no mechanism in the x-y plane; however, it has a mechanism whereby the free node #3 can move out of the x-y plane. The structure has one state of self-stress consisting of the two cross-elements in compression and the outer elements in tension, or vice versa. The structure is prestress-stable when the two cross-elements are in compression and the four outer elements are in tension.

In this example, prestress is applied directly through actuation, thus the *eigenstrain* \mathbf{e}_0 is denoted as the actuator length change $\Delta \mathbf{L}_0$. In prestress design (Eq. 32, Step 2), $\Delta \mathbf{L}_0$ for elements 1-4 are constrained to be zero (because they are not active) and $\Delta \mathbf{L}_0$ for elements 5 and 6 are required to be identical. In addition, the upper bound for $\Delta \mathbf{L}_0$ is set to 5 mm. The prestress \mathbf{F}_0 and related product force \mathbf{G} allow to build the IFME governing matrix \mathbf{S}^* . Element forces (Step 3) and nodal displacement (Step 4) are computed following the IFME analysis process outlined in Section 5.5.

The prestress \mathbf{F}_0 together with the initial nodal displacement \mathbf{U}_0 caused by $\Delta \mathbf{L}_0$ are given in Table 7.

Table 7 Prestress \mathbf{F}_0 and nodal displacement \mathbf{U}_0 caused by $\Delta \mathbf{L}_0$

Element forces (kN)						Nodal displacements (mm)					
1	2	3	4	5	6	2-x	3-x	4-x	3-y	4-y	3-z
49.25	49.25	49.25	49.25	-69.65	-69.65	2.91	2.91	0.00	2.91	2.91	0.00

The element forces \mathbf{F}_{load} and nodal displacements \mathbf{U}_{load} caused by the external load \mathbf{P} are given in Table 8.

Table 8 Element force \mathbf{F}_{load} and nodal displacement \mathbf{U}_{load} caused by external load

Element forces (kN)						Nodal displacements (mm)					
1	2	3	4	5	6	2-x	3-x	4-x	3-y	4-y	3-z
0.09	0.09	0.09	0.09	1.29	-0.13	0.01	0.02	0.01	0.01	0.01	20.30

The final element forces and nodal displacements (Table 9) are the sum of those caused by $\Delta\mathbf{L}_0$ (Table 7) and those caused by the external load \mathbf{P} (Table 8). Results are practically identical with those obtained by using the method based on SFM [35] and DM [36].

Table 9 Total element force \mathbf{F} and nodal displacement \mathbf{U}

Element force change (kN)						Nodal displacements change (mm)					
1	2	3	4	5	6	2-x	3-x	4-x	3-y	4-y	3-z
49.34	49.34	49.34	49.34	-68.36	-69.78	2.92	2.93	0.01	2.92	2.92	20.30

All element forces are within required limits for the admissible stress and buckling. However, the displacement corresponding to the mechanism (3-z) is 20.30 mm which is beyond the required limit. Therefore, a further actuation step is employed to reduce the displacement within the required limit. Assume a $\Delta\mathbf{L} = 6$ mm for the bracing elements, the element force change is $\Delta\mathbf{F}_{control}$. The element force and nodal displacement after control is given by

$$\begin{aligned}\mathbf{F}_{control} &= \mathbf{F}_0 + \mathbf{F}_{load} + \Delta\mathbf{F}_{control} \\ \mathbf{U}_{control} &= \mathbf{U}_0 + \mathbf{U}_{load} + \Delta\mathbf{U}_{control}\end{aligned}\quad 62$$

The product force matrix is updated using \mathbf{F} through Eq. 25 and subsequently the IFME governing matrices are updated. The element forces and nodal displacements after control are given in Table 10.

Table 10 Element force ($\mathbf{F}_{control}$) and nodal displacement ($\mathbf{U}_{control}$) after control

Element forces (kN)						Nodal displacements (mm)					
1	2	3	4	5	6	2-x	3-x	4-x	3-y	4-y	3-z
108.44	108.44	108.44	108.44	-151.95	-151.36	6.40	6.41	0.01	6.40	6.40	9.23

The actuator length changes are determined a-priori and thus they might not be optimal in terms of control efficacy. Nonetheless, through control, all element forces and nodal displacements are within required limits. Some of the element forces and nodal displacements increase significantly compared to those before control. The computation of displacements in a prestress-stable kinematically indeterminate structure depends on the stiffness of the mechanism. The control process adopted here can be thought of as a further prestress which increases the force in the elements as well as the stiffness of the mechanism. For this reason, the displacement corresponding to the mechanism decreases. However, for compatibility (Eq.

18) the non-elastic change of length $\Delta\mathbf{L}$ also causes an increase in some of the displacements after control.

The element forces and nodal displacements after control obtained through the SVD-FM are given in Table 11. It can be seen that the displacement corresponding to the mechanism does not change after control; this is because the SVD-FM does not consider the change of the stiffness of the mechanism caused by prestress (in this case produced by actuation).

Table 11 Element force ($\mathbf{F}_{control}^{SVD-FM}$) and nodal displacement ($\mathbf{U}_{control}^{SVD-FM}$) after control

Element forces (kN)						Nodal displacements (mm)					
1	2	3	4	5	6	2-x	3-x	4-x	3-y	4-y	3-z
108.44	108.44	108.44	108.44	-151.95	-151.36	6.40	6.41	0.01	6.40	6.40	20.30

7 Discussion

The IFM was proposed nearly half a century ago and so far it could not be applied to the analysis of kinematically indeterminate systems because it does not model the effect of prestress on the stiffness of inextensional mechanisms. This paper gives a reformulation and extension of the IFM, here named Extended Integrated Force Method (IFME) which is able to predict the response of prestress-stable kinematically indeterminate systems with single and multiple self-stress states and under arbitrary loading. Compared to other force methods, the IFME has some unique advantages.

7.1 IFME vs SFM

The IFME adopts the concept of product force to model the stiffness of inextensional mechanisms stabilized through prestress similarly to the procedure given in [14, 35] which is based on the SFM. However, the SFM requires the choice of redundant elements to determine a statically determinate basis structure and therefore it is not suitable for automation and it does not generalize well. As concluded by Patnaik [30]: “*The IFM is the true force method. The SFM can, at best, be considered as a solution technique of the IFM for static analysis, and the IFM bypasses the popular concepts of redundants and basis determinant structure of the SFM.*”

7.2 IFME vs SVD-FM

The SVD-FM proposed in [28] is based on the SVD of the equilibrium matrix, and therefore it can only deal with the situations in which equilibrium conditions are described completely by Eq. 1. However, as explained in Section 4, if the external load contains components lying in the left-null space of the equilibrium matrix (i.e. loads that excite one or more mechanism modes), Eq. 1 does not admit any solution. In these situations, SVD-FM cannot produce accurate solutions, which has been verified through the numerical examples given in section 6. This is because the SVD-FM does not consider the effect of prestress on the stiffness of the mechanism. In fact, SVD-FM can be proved to be identical to a reduced form of the IFME which does not include the product force, see Appendix A.2.

7.3 IFME vs IFM

Compared to the IFM, the major improvement of the IFME is the incorporation of the product force which allows to compute the structural response of prestress-stable kinematically indeterminate systems. For the computation of forces, the IFME is similar to the IFM (compare Eq. 35 with Eq. 7). However, for the computation of displacements, the IFME uses directly the compatibility matrix in Eq. 46 which has a more intuitive physical meaning than Eq. 11. In addition, Eq. 46 also applies to the computation of displacements for kinematically determinate systems as explained in Appendix A.3. That is, Eq. 11 in the original IFM can be replaced by Eq. 46. Therefore, compared to the IFM, the IFME not only applies to the analysis of prestress-stable kinematically indeterminate systems but it also uses a simpler formulation to compute the displacements for systems with or without kinematically indeterminacy.

7.4 IFME vs DM

The displacement method (DM) has been successfully applied to linear analysis of prestress-stable kinematically indeterminate systems. The main steps of the DM are given in the block diagram shown in Figure 9. The comparison between IFME and DM focuses on the analysis of statically and kinematically indeterminate structures and therefore the prestress design process (Step 2) is included also in the DM workflow. With respect to the IFME, the order of force and displacement computation is inverted which is a common difference between force and displacement methods. For comparison with the IFME, the external load for the DM is extended with the term $\mathbf{AB}^{-1}\mathbf{e}_0$ to include the effect of *eigenstrain* \mathbf{e}_0 . The effect of \mathbf{e}_0 is equivalent to that of a force parallel to the axis of the corresponding element and applied to

its end nodes. Comparing with the IFME block diagram in Figure 1, it is clear that all operations in both methods can be fully automated.

Before carrying out an analysis for a given external load \mathbf{P} , the key step in the DM is to assemble the tangent stiffness matrix $\mathbf{K} \in \mathbb{R}^{n^f \times n^f}$ which consists of material stiffness $\mathbf{K}_m \in \mathbb{R}^{n^f \times n^f}$ and geometric stiffness $\mathbf{K}_g \in \mathbb{R}^{n^f \times n^f}$. In the IFME the same step is to assemble the governing matrix $\mathbf{S}^* \in \mathbb{R}^{(n^e+m) \times (n^e+m)}$. Since $n^e + m = n^f + s$, the dimension of \mathbf{S}^* can also be expressed as $\mathbf{S}^* \in \mathbb{R}^{(n^f+s) \times (n^f+s)}$.

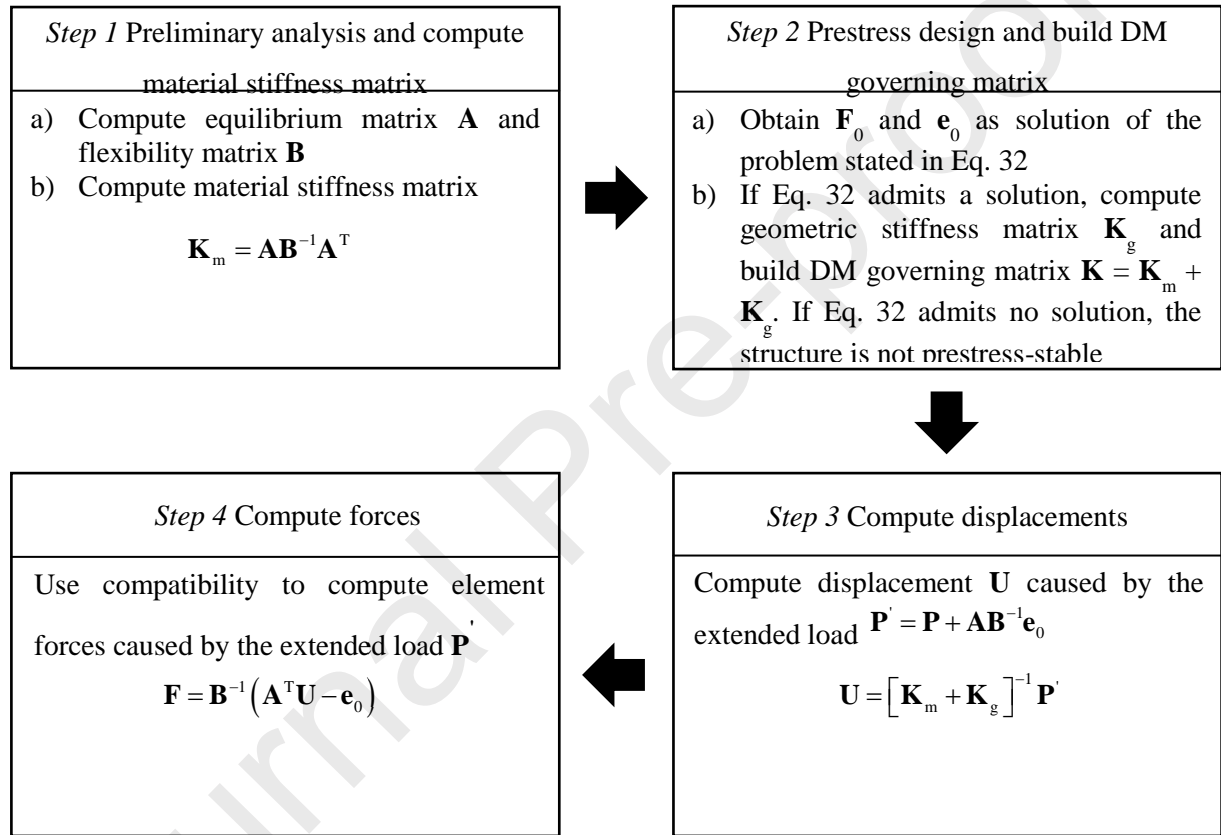


Figure 9 DM analysis process

The main differences between IFME and DM governing matrices are:

1. The difference between the dimensions of $\mathbf{S}^* \in \mathbb{R}^{(n^f+s) \times (n^f+s)}$ and $\mathbf{K} \in \mathbb{R}^{n^f \times n^f}$ depends on the number of self-stress states s
2. \mathbf{S}^* is not symmetric, whereas the tangent stiffness matrix \mathbf{K} is symmetric
3. \mathbf{S}^* is sparser than tangent stiffness matrix \mathbf{K}
4. \mathbf{S}^* is a better conditioned matrix than the tangent stiffness matrix \mathbf{K}

From point #1, it follows that for prestress-stable kinematically indeterminate structures, \mathbf{S}^* has higher dimensions than \mathbf{K} because $s > 0$. Point 3 regarding the sparsity of \mathbf{S}^* was already mentioned by Patnaik et al. [40] for the IFM governing matrix. The same applies to IFME because the inclusion of the product force \mathbf{G} does not change the main body of \mathbf{S}^* which is the equilibrium matrix \mathbf{A} . Referring to Example 3, the density of \mathbf{S}^* is 24.3% while that of \mathbf{K} is 45.6%. Point #4 was also highlighted in [40] regarding the conditioning of the IFM governing matrix. The same applies to IFME because, generally, the condition number of \mathbf{S}^* is much smaller than that of \mathbf{K} . Referring to Example 3, the condition number of \mathbf{S}^* is 99.8 while that of \mathbf{K} is 9.6172×10^3 .

With regard to computational complexity, the most demanding operations for IFME and DM are given in Table 12. For both methods the computational complexity depends on the inherent characteristics of the structure, i.e. n^e , n^f , s , and m . However, the computational complexity of the IFME is governed by the SVD of \mathbf{A} , while that of the DM is governed by the computation of material and geometric stiffness matrices \mathbf{K}_m and \mathbf{K}_g as well as the inversion of the tangent stiffness matrix \mathbf{K} .

Table 12 Computational complexity of IFME vs DM

Method	Operation	Computational complexity	Example 3
IFME	SVD of \mathbf{A}	$O\left(n^f (n^e)^2 + n^e (n^f)^2\right)$	$O(2 \times 30^3) = 54000$
	$\mathbf{F}^* = [\mathbf{S}^*]^{-1} \mathbf{P}^*$	$O\left((n^f + s)^3\right)$	$O((30 + 3)^3) = 35937$
DM	$\mathbf{K}_m = \mathbf{A}\mathbf{B}^{-1}\mathbf{A}^T$	$O\left(\max\left\{n^e (n^f)^2, n^f (n^e)^2\right\}\right)$	$O(30^3) = 27000$
	$\mathbf{K}_g = \mathbf{I} \otimes (\mathbf{D}^T \mathbf{Q} \mathbf{D})$	$O\left(\max\left\{n^e (n^f)^2, n^f (n^e)^2\right\}\right)$	$O(30^3) = 27000$
	$\mathbf{U} = (\mathbf{K}_m + \mathbf{K}_g)^{-1} \mathbf{P}$	$O\left((n^f)^3\right)$	$O(30^3) = 27000$

In general, the computational complexity of IFME and DM is comparable as they are both third degree polynomial $O(n^3)$. From point #1 and point #2 it follows that for prestress-stable kinematically indeterminate structures, the inversion of \mathbf{K} requires less operations than that of \mathbf{S}^* . However, with respect to \mathbf{K} , generally, \mathbf{S}^* has a lower density (i.e. it is sparser)

which makes it more efficient in terms of data storage and it has a lower condition number which results in a higher accuracy of the inverse and, importantly, of the structure response.

As a final remark, the IFME produces more information than the DM because the total displacement \mathbf{U} is decoupled into an extensional \mathbf{U}_e and inextensional \mathbf{U}_k part, which gives a deeper insight into the response of the structure.

7.5 Nonlinear response

The formulation presented in this paper is given within the assumption of small strains and small displacements. The prestress is assumed not to change after an infinitesimal mechanism is excited because mechanisms are assumed to cause no first order deformation of the elements. However, it should be noted that the displacement caused by an infinitesimal mechanism might be significantly large and thus it might cause a significant deformation of the elements. In these situations, the constant prestress assumption generally gives an overestimation of the displacements caused by an infinitesimal mechanism. Within the small strain assumption, second order deformations are ignored and therefore, generally, the stiffness of infinitesimal mechanisms is underestimated. Accuracy could be improved by considering second-order effects for the element length changes [35], i.e. geometric nonlinearity, which could be the subject of future work.

8 Conclusion

This paper offers a new extension of the Integrated Force Method (IFM) to the analysis of prestress-stable statically and kinematically indeterminate systems. The Extended Integrated Force Method (IFME) is a systematic and general approach to structural analysis which can be also applied to kinematically determinate systems.

This paper has shown that the IFME is an efficient tool for linear analysis of prestress-stable statically and kinematically indeterminate systems such as cable-domes, cable-nets and tensegrity structures. Compared to the better known Displacement Method (DM), the IFME is a suitable alternative and it offers a deeper insight into the structure response which is decoupled into an extensional and an inextensional part for prestress-stable kinematically indeterminate systems. Compared to other force methods, the IFME has some unique advantages including ease of automation, the ability to model the stiffness of infinitesimal mechanisms stabilized through prestress and an intuitive formulation which has a clear physical interpretation. In addition, this work has shown that the IFME is a convenient tool

for the simulation of force and shape control of kinematically indeterminate adaptive structures under static loading.

Future work could investigate the application of the IFME to carry out stability analysis and to compute the dynamic response of prestress-stable kinematically indeterminate structures. Future work could also look into applications of the IFME to integrated structure-control design for kinematically indeterminate adaptive structures.

Acknowledgements

The authors thankfully acknowledge Swiss National Science Foundation who provided core funding for this research via project *Structural Adaptation through Large Shape Changes* (200021_182033).

Appendix A

A.1 SVD-FM formulation

The key equations of the SVD-FM are given in this section. Element forces are computed as

$$\mathbf{F} = (\mathbf{W}_r \mathbf{V}_r^{-1} \mathbf{U}_r^T) \mathbf{P} + \mathbf{W}_s \boldsymbol{\eta}, \quad 63$$

where $\boldsymbol{\eta}$ is given by

$$\boldsymbol{\eta} = -(\mathbf{W}_s^T \mathbf{B} \mathbf{W}_s)^{-1} \mathbf{W}_s^T [\mathbf{B} (\mathbf{W}_r \mathbf{V}_r^{-1} \mathbf{U}_r^T) \mathbf{P} + \mathbf{e}_0]. \quad 64$$

The displacements are computed as

$$\mathbf{U} = \mathbf{U}_r \mathbf{V}_r^{-1} \mathbf{W}_r^T (\mathbf{B} \mathbf{F} + \mathbf{e}_0) + \mathbf{U}_m \boldsymbol{\gamma}. \quad 65$$

All terms have already been defined in Section 2 and Section 3. A detailed formulation of the SVD-FM is given in [28].

A.2 Equivalence of the SVD-FM with the reduced form of the IFME

The IFME governing Eq. 35 reduces to a similar form of the IFM governing Eq. 7 if the product force matrix \mathbf{G} is taken out. In this case the governing matrix reduces to $\mathbf{S} \in \mathbb{R}^{(n^e+m) \times n^e}$. When the structure is kinematically indeterminate, because of the existence of mechanisms ($m > 0$), \mathbf{S} is not a square matrix with full rank but a rectangular matrix with full column rank, therefore Eq. 10 cannot be used to calculate the element forces. Instead of using the inverse of the governing matrix \mathbf{S} , the Moore-Penrose pseudoinverse \mathbf{S}^+ could be used to obtain a unique solution. That is

$$\mathbf{F} = \mathbf{S}^+ \mathbf{P}^*. \quad 66$$

Next, we prove that the element forces obtained through Eq. 66 are identical to those obtained through the SVD-FM, i.e. Eq. 66 is equivalent to Eq. 63. The proof is based on Lemma 1, which gives the decomposition of a Moore-Penrose pseudoinverse of a vertically partitioned rectangular matrix [48]. Note that the first part of the proof below was given in [38] and it is reported in this paper for completeness.

Proof:

Lemma 1. If $\mathbf{C} \in \mathbb{R}^{p \times n}$ and $\mathbf{D} \in \mathbb{R}^{q \times n}$ then:

$$\begin{bmatrix} \mathbf{C} \\ \mathbf{D} \end{bmatrix}^+ = \begin{bmatrix} \mathbf{C}^+ - \xi \mathbf{D} \mathbf{C}^+ \\ \xi \end{bmatrix}$$

where

$$\xi = (\mathbf{I} - \mathbf{C}^+ \mathbf{C}) [\mathbf{D} (\mathbf{I} - \mathbf{C}^+ \mathbf{C})]^+$$

Through Lemma 1 and considering Eq. 9, Eq. 66 can be expanded as

$$\mathbf{F} = \begin{bmatrix} \mathbf{A}^+ - \xi (\mathbf{W}_s^T \mathbf{B}) \mathbf{A}^+ \\ \xi \end{bmatrix} \begin{bmatrix} \mathbf{P} \\ -\mathbf{W}_s^T \mathbf{e}_0 \end{bmatrix}, \quad 67$$

where

$$\xi = (\mathbf{I} - \mathbf{A}^+ \mathbf{A}) [\mathbf{W}_s^T \mathbf{B} (\mathbf{I} - \mathbf{A}^+ \mathbf{A})]^+ . \quad 68$$

Through the identity $\mathbf{I} - \mathbf{A}^+ \mathbf{A} = \mathbf{W}_s \mathbf{W}_s^T$ [49], ξ can be rewritten as

$$\xi = \mathbf{W}_s \mathbf{W}_s^T (\mathbf{W}_s^T \mathbf{B} \mathbf{W}_s \mathbf{W}_s^T)^+ . \quad 69$$

Since $\mathbf{W}_s \mathbf{W}_s^T (\mathbf{W}_s^T)^+ = \mathbf{W}_s$ [49], and owing to the fact that $\mathbf{W}_s^T \mathbf{B} \mathbf{W}_s$ is an invertible matrix, ξ can be rearranged into

$$\xi = \mathbf{W}_s (\mathbf{W}_s^T \mathbf{B} \mathbf{W}_s)^{-1} . \quad 70$$

Expanding Eq. 67 and replacing ξ with Eq. 70 gives

$$\mathbf{F} = \begin{bmatrix} \mathbf{A}^+ - \mathbf{W}_s (\mathbf{W}_s^T \mathbf{B} \mathbf{W}_s)^{-1} (\mathbf{W}_s^T \mathbf{B}) \mathbf{A}^+ \\ \mathbf{W}_s (\mathbf{W}_s^T \mathbf{B} \mathbf{W}_s)^{-1} \mathbf{W}_s^T \mathbf{e}_0 \end{bmatrix} \mathbf{P} - \mathbf{W}_s (\mathbf{W}_s^T \mathbf{B} \mathbf{W}_s)^{-1} \mathbf{W}_s^T \mathbf{e}_0 . \quad 71$$

Using the identity $\mathbf{A}^+ = \mathbf{W}_r \mathbf{V}_r^{-1} \mathbf{U}_r^T$ [49], and then tidying up

$$\mathbf{F} = (\mathbf{W}_r \mathbf{V}_r^{-1} \mathbf{U}_r^T) \mathbf{P} - \mathbf{W}_s (\mathbf{W}_s^T \mathbf{B} \mathbf{W}_s)^{-1} \mathbf{W}_s^T [\mathbf{B} (\mathbf{W}_r \mathbf{V}_r^{-1} \mathbf{U}_r^T) \mathbf{P} + \mathbf{e}_0] . \quad 72$$

Finally, \mathbf{F} can be expressed as

$$\mathbf{F} = (\mathbf{W}_r \mathbf{V}_r^{-1} \mathbf{U}_r^T) \mathbf{P} + \mathbf{W}_s \boldsymbol{\eta}, \quad 73$$

where

$$\boldsymbol{\eta} = -(\mathbf{W}_s^T \mathbf{B} \mathbf{W}_s)^{-1} \mathbf{W}_s^T [\mathbf{B}(\mathbf{W}_r \mathbf{V}_r^{-1} \mathbf{U}_r^T) \mathbf{P} + \mathbf{e}_0]. \quad 74$$

Eq. 73 is identical to Eq. 63, thus Eq. 66 is equivalent to Eq. 63. Note that the force \mathbf{F} obtained through Eq. 63 (or Eq. 66) can only equilibrate external loads whose components lie in the column space of the equilibrium matrix i.e. with loads that do not excite any mechanism mode.

For the computation of displacements, if the product force is not considered, Eq. 46 reduces to

$$\mathbf{A}^T \mathbf{U}_e = \mathbf{B} \mathbf{F} + \mathbf{e}_0. \quad 75$$

For a prestress-stable kinematically indeterminate system, the matrix \mathbf{A}^T is singular (it is rank deficient column wise and row wise), therefore, the extensional displacement \mathbf{U}_e cannot be uniquely determined through Eq. 75. By using the Moore-Penrose pseudoinverse of matrix \mathbf{A}^T , \mathbf{U}_e can be expressed as [44]

$$\mathbf{U}_e = (\mathbf{A}^T)^+ (\mathbf{B} \mathbf{F} + \mathbf{e}_0) + (\mathbf{I} - (\mathbf{A}^T)^+ \mathbf{A}^T) \boldsymbol{\omega} \quad 76$$

where $\boldsymbol{\omega}$ is an arbitrary combination coefficient vector. Through the identities $(\mathbf{A}^T)^+ = (\mathbf{A}^+)^T$ and $\mathbf{I} - (\mathbf{A}^T)^+ \mathbf{A}^T = \mathbf{U}_m \mathbf{U}_m^T$ [49], Eq. 76 can be written as

$$\mathbf{U}_e = \mathbf{U}_r \mathbf{V}_r^{-1} \mathbf{W}_r^T (\mathbf{B} \mathbf{F} + \mathbf{e}_0) + \mathbf{U}_m \mathbf{U}_m^T \boldsymbol{\omega}. \quad 77$$

Let $\mathbf{U}_m^T \boldsymbol{\omega} = \boldsymbol{\gamma}$, then

$$\mathbf{U}_e = \mathbf{U}_r \mathbf{V}_r^{-1} \mathbf{W}_r^T (\mathbf{B} \mathbf{F} + \mathbf{e}_0) + \mathbf{U}_m \boldsymbol{\gamma}, \quad 78$$

Eq. 78 is identical to Eq. 65, thus Eq. 75 is equivalent to Eq. 65. For a prestress-stable kinematically indeterminate system, $\boldsymbol{\gamma}$ can be determined through the orthogonality between \mathbf{U}_e and product force matrix \mathbf{G} , i.e. Eq. 45. Note that the displacement obtained through Eq. 65 (or through Eq. 75) only accounts for the part caused by load components that lie in the column space of the equilibrium matrix i.e. loads that can be taken by the system in its initial configuration. That is, \mathbf{U}_e might contain contributions from mechanism modes. However, the inextensional part in \mathbf{U}_e is not caused by load components that lie in the left null space of the equilibrium matrix. For brevity, since \mathbf{U}_k (see Section 4.2) contains only inextensional components of the displacement, \mathbf{U}_e has been denoted as extensional in the IFME formulation (Section 5).

In addition, Eq. 75 also applies to kinematically determinate systems ($m = 0$) in which the transpose of the equilibrium matrix \mathbf{A}^T has full column rank thus $\mathbf{I} = (\mathbf{A}^T)^+ \mathbf{A}^T$. For this reason, the displacement \mathbf{U} in a kinematically determinate system can be directly calculated as

$$\mathbf{U} = (\mathbf{A}^T)^+ (\mathbf{BF} + \mathbf{e}_0). \quad 79$$

■

A.3 Equivalence of the IFM to the reduced IFME for the analysis of kinematically determinate systems

For a kinematically determinate system ($m = 0$), the product force matrix \mathbf{G} does not exist, thus the governing equation Eq. 35 of the IFME reduces to Eq. 7, which proves immediately the equivalence of the governing equations of the two methods for kinematically determinate systems.

For the calculation of displacements, in order to show that Eq. 79 is equivalent to Eq. 11, it is sufficient to prove that $\mathbf{J} = (\mathbf{A}^T)^+$. Recalling Lemma 1 in Eq. 67, Eq. 11 can be rewritten as

$$\mathbf{U} = \left[\mathbf{A}^+ - \xi (\mathbf{W}_s^T \mathbf{B}) \mathbf{A}^+ \quad \vdots \quad \xi \right]^T (\mathbf{BF} + \mathbf{e}_0), \quad 80$$

where ξ is given by Eq. 68. Expanding Eq. 80 and replacing ξ with Eq. 68 gives

$$\mathbf{U} = \left[\mathbf{A}^+ - \mathbf{W}_s (\mathbf{W}_s^T \mathbf{B} \mathbf{W}_s)^{-1} (\mathbf{W}_s^T \mathbf{B}) \mathbf{A}^+ \quad \vdots \quad \mathbf{W}_s (\mathbf{W}_s^T \mathbf{B} \mathbf{W}_s)^{-1} \right]^T (\mathbf{BF} + \mathbf{e}_0). \quad 81$$

By taking the first n^d rows of $(\mathbf{S}^{-1})^T$, \mathbf{J} can be expressed as

$$\mathbf{J} = \left[\mathbf{A}^+ - \mathbf{W}_s (\mathbf{W}_s^T \mathbf{B} \mathbf{W}_s)^{-1} (\mathbf{W}_s^T \mathbf{B}) \mathbf{A}^+ \right]^T. \quad 82$$

Substituting Eq. 82 into Eq. 11

$$\mathbf{U} = \left[\mathbf{A}^+ - \mathbf{W}_s (\mathbf{W}_s^T \mathbf{B} \mathbf{W}_s)^{-1} (\mathbf{W}_s^T \mathbf{B}) \mathbf{A}^+ \right]^T (\mathbf{BF} + \mathbf{e}_0). \quad 83$$

Considering the compatibility conditions in Eq. 3 $\mathbf{W}_s^T (\mathbf{e}_0 + \mathbf{BF}) = \mathbf{0}$, the terms containing \mathbf{W}_s^T vanish and therefore Eq. 83 reduces to

$$\mathbf{U} = (\mathbf{A}^+)^T (\mathbf{BF} + \mathbf{e}_0). \quad 84$$

Eq. 84 is equivalent to Eq. 11 and since $(\mathbf{A}^T)^+ = (\mathbf{A}^+)^T$ Eq. 79 is equivalent to Eq. 11. ■

Journal Pre-proofs

References

- [1] S. P. Timoshenko and D. H. Young, *Theory of Structures*, 2 ed., New York: McGraw-Hill, 1965.
- [2] X. F. Yuan and S. L. Dong, "Integral feasible prestress of cable domes," *Computers & structures*, vol. 81, no. 21, pp. 2111-2119, 2003.
- [3] X. Yuan, L. Chen and S. Dong, "Prestress design of cable domes with new forms," *International Journal of Solids and Structures*, vol. 44, no. 9, pp. 2773-2782, 2007.
- [4] A. Nenadović, "Development, characteristics and comparative structural analysis of tensegrity type cable domes," *Spatium*, no. 22, pp. 57-66, 2010.
- [5] S. Dhakal, N. P. Bhandary, R. Yatabe and N. Kinoshita, "Experimental, numerical and analytical modelling of a newly developed rockfall protective cable-net structure," *Natural Hazards and Earth System Sciences*, vol. 11, no. 12, pp. 3197-3212, 2011.
- [6] P. Jiang, Q. M. Wang and Q. Zhao, "Optimization and analysis on cable net structure supporting the reflector of the large radio telescope FAST," in *Applied Mechanics and Materials*, 2011.
- [7] R. Torsing, J. Bakker, R. Jansma and D. Veenendaal, "Large-scale designs for mixed fabric and cable net formed structures," in *Proceedings of the 2nd international conference on flexible formworks, Bath, UK*. <http://www.block.arch.ethz.ch/brg/project/hilo-research-innovation-unit-nest>, 2012.
- [8] G. Tibert, "Deployable tensegrity structures for space applications," KTH, 2002.
- [9] K. Franklin, E. Ozkan, D. Powell and others, "Design of the Kurilpa Pedestrian Bridge for Dynamic Effects Due to Pedestrian and Wind Loads," in *5th Civil Engineering Conference in the Asian Region and Australasian Structural Engineering Conference 2010, The, 2010*.
- [10] L. Rhode-Barbarigos, N. B. H. Ali, R. Motro and I. F. C. Smith, "Designing tensegrity modules for pedestrian bridges," *Engineering Structures*, vol. 32, no. 4, pp. 1158-1167, 2010.
- [11] T. Tarnai, "Simultaneous static and kinematic indeterminacy of space trusses with cyclic symmetry," *International Journal of Solids and Structures*, vol. 16, pp. 347-359, 1980.
- [12] S. Pellegrino and C. R. Calladine, "Matrix analysis of statically and kinematically indeterminate frameworks," *International Journal of Solids and Structures*, vol. 22, no. 4, pp. 409-428, 1986.
- [13] R. Connelly and W. Whiteley, "Second-order rigidity and prestress stability for tensegrity frameworks," *SIAM Journal on Discrete Mathematics*, vol. 9, no. 3, pp. 453-491, 1996.
- [14] C. R. Calladine and S. Pellegrino, "First-order infinitesimal mechanisms," *International Journal of Solids and Structures*, vol. 27, no. 4, pp. 505-515, 1991.
- [15] E. N. Kuznetsov, "On immobile kinematic chains and a fallacious matrix analysis," *Trans. ASME, J. Appl. Mech.*, vol. 56, pp. 222-224, 1989.
- [16] T. Tarnai and J. Szabó, "Rigidity and stability of prestressed infinitesimal mechanisms," in *New Approaches to Structural Mechanics, Shells and Biological Structures*, Springer, 2002, pp. 245-256.
- [17] S. El-Lishani, H. Nooshin and P. Disney, "Investigating the statical stability of pin-jointed structures using genetic algorithm," *International Journal of Space Structures*, vol. 20, no. 1, pp. 53-68, 2005.
- [18] X. Xu and Y. Luo, "Force finding of tensegrity systems using simulated annealing algorithm," *Journal of structural engineering*, vol. 136, no. 8, pp. 1027-1031, 2010.
- [19] Y. Chen, J. Feng and Y. Wu, "Prestress stability of pin-jointed assemblies using ant colony systems," *Mechanics Research Communications*, vol. 41, pp. 30-36, 2012.
- [20] Y. Wang and X. Xu, "Prestress Design of Tensegrity Structures Using Semidefinite Programming," *Advances in Civil Engineering*, vol. 2019, 2019.
- [21] O. C. Zienkiewicz, R. L. Taylor, P. Nithiarasu and J. Z. Zhu, *The finite element method*, vol. 3, McGraw-hill London, 1977.
- [22] J. S. Przemieniecki and Przemieniecki, *Theory of matrix structural analysis*, vol. 1, McGraw-Hill New York, 1968.
- [23] R. K. Livesley, *Matrix methods of structural analysis*, Pergamon, 1975.
- [24] I. Kaneko, M. Lawo and G. Thierauf, "On computational procedures for the force method," *International Journal for Numerical Methods in Engineering*, vol. 18, no. 10, pp. 1469-1495, 1982.
- [25] S. Patnaik, "An integrated force method for discrete analysis," *International Journal for Numerical Methods in Engineering*, vol. 6, no. 2, pp. 237-251, 1973.

- [26] S. N. Patnaik, R. M. Coroneos and D. A. Hopkins, "Recent advances in the method of forces: integrated force method of structural analysis," *Advances in Engineering Software*, vol. 29, no. 3-6, pp. 463-474, 1998.
- [27] S. N. Patnaik, D. A. Hopkins and G. R. Halford, "Integrated force method solution to indeterminate structural mechanics problems," 2004.
- [28] S. Pellegrino, "Structural computations with the singular value decomposition of the equilibrium matrix," *International Journal of Solids and Structures*, vol. 30, no. 21, pp. 3025-3035, 1993.
- [29] S. Timoshenko, *History of Strength of Materials*, New York: McGraw-Hill, 1953.
- [30] S. N. Patnaik, "The integrated force method versus the standard force method," *Computers & structures*, vol. 22, no. 2, pp. 151-163, 1986.
- [31] S. N. Patnaik and S. Yadagiri, "Frequency analysis of structures by integrated force method," *Journal of Sound and Vibration*, vol. 83, no. 1, pp. 93-109, 1982.
- [32] R. Sedaghati, "Benchmark case studies in structural design optimization using the force method," *International Journal of Solids and Structures*, vol. 42, no. 21-22, pp. 5848-5871, 2005.
- [33] S. N. Patnaik, A. S. Gendy, L. Berke and D. A. Hopkins, "Modified fully utilized design (MFUD) method for stress and displacement constraints," *International Journal for Numerical Methods in Engineering*, vol. 41, no. 7, pp. 1171-1194, 1998.
- [34] G. Senatore, P. Duffour and P. Winslow, "Synthesis of minimum energy adaptive structures," *Structural and Multidisciplinary Optimization*, vol. 60, no. 3, pp. 849-877, 2019.
- [35] S. Pellegrino, "Analysis of prestressed mechanisms," *International Journal of Solids and Structures*, vol. 26, no. 12, pp. 1329-1350, 1990.
- [36] S. Guest, "The stiffness of prestressed frameworks: a unifying approach," *International Journal of Solids and Structures*, vol. 43, no. 3-4, pp. 842-854, 2006.
- [37] S. D. Guest, "The stiffness of tensegrity structures," *IMA Journal of Applied Mathematics*, vol. 76, no. 1, pp. 57-66, 2010.
- [38] A. P. Reksowardojo and G. Senatore, "A proof of equivalence of two force methods for active structural control," *Mechanics Research Communications*, vol. 103, p. 103465, 2020.
- [39] F. Ziegler, "Computational aspects of structural shape control," *Computer & Structures*, vol. 83, pp. 1191-1204, 2005.
- [40] S. N. Patnaik, L. Berke and R. H. Gallagher, "Integrated force method versus displacement method for finite element analysis," *Computers & Structures*, vol. 38, no. 4, pp. 377-407, 1991.
- [41] R. Connelly, "Tensegrity structures: why are they stable?," in *Rigidity theory and applications*, Springer, 2002, pp. 47-54.
- [42] F. Alizadeh, J.-P. A. Haerberly and M. L. Overton, "Primal-dual interior-point methods for semidefinite programming: convergence rates, stability and numerical results," *SIAM Journal on Optimization*, vol. 8, no. 3, pp. 746-768, 1998.
- [43] C. R. Calladine, "Modal stiffnesses of a pretensioned cable net," *International Journal of Solids and Structures*, vol. 18, no. 10, pp. 829-846, 1982.
- [44] R. Penrose, "A generalized inverse for matrices," in *Mathematical proceedings of the Cambridge philosophical society*, 1955.
- [45] R. Levy and W. R. Spillers, *Analysis of geometrically nonlinear structures*, Springer Science & Business Media, 2013.
- [46] Y. Luo and J. Lu, "Geometrically non-linear force method for assemblies with infinitesimal mechanisms," *Computers & structures*, vol. 84, no. 31-32, pp. 2194-2199, 2006.
- [47] R. E. Skelton and M. C. de Oliveira, *Tensegrity systems*, vol. 1, New York: Springer, 2009.
- [48] D. A. Harville, *Matrix algebra from a statistician's perspective*, Taylor & Francis Group, 1998.
- [49] K. B. Petersen, M. S. Pedersen and others, "The matrix cookbook," *Technical University of Denmark*, vol. 7, no. 15, p. 510, 2008.